

RESEARCH ARTICLE

# Multifunctional 3D platforms for rapid hemostasis and wound healing: Structural and functional prospects at biointerfaces

Keya Ganguly,<sup>1†</sup> Maria Mercedes Espinal,<sup>1†</sup> Sayan Deb Dutta,<sup>1</sup> Dinesh K. Patel,<sup>3</sup> Tejal V. Patil,<sup>1,2</sup> Rachmi Luthfikasari,<sup>1</sup> Ki-Taek Lim<sup>1,2,3\*</sup>

<sup>1</sup>Department of Biosystems Engineering, Kangwon National University, Chuncheon 24341, Republic of Korea

<sup>2</sup>Interdisciplinary Program in Smart Agriculture, Kangwon National University, Chuncheon 24341, Republic of Korea

<sup>3</sup>Institute of Forest Science, Kangwon National University, Chuncheon 24341, Republic of Korea

(This article belongs to the *Special Issue: Advances in 3D bioprinting for regenerative medicine and drug screening*)

## Abstract

Fabrication of multifunctional hemostats is indispensable against chronic blood loss and accelerated wound healing. Various hemostatic materials that aid wound repair or rapid tissue regeneration has been developed in the last 5 years. This review provides an overview of the three-dimensional (3D) hemostatic platforms designed through the latest technologies like electrospinning, 3D printing, and lithography, solely or in combination, for application in rapid wound healing. We critically discuss the pivotal role of micro/nano-3D topography and biomaterial properties in mediating rapid blood clots and healing at the hemostat-biointerface. We also highlight the advantages and limitations of the designed 3D hemostats. We anticipate that this review will guide the fabrication of smart hemostats of the future for tissue engineering applications.

**Keywords:** Multifunctional hemostats; Wound healing; Micro/nano-3D topography; Hemostat-biointerface; Tissue engineering

†These authors contributed equally to this work.

**\*Corresponding author:**

Ki-Taek Lim (ktlim@kangwon.ac.kr)

**Citation:** Ganguly K, Espinal MM, Dutta SD, et al., 2023, Multifunctional 3D platforms for rapid hemostasis and wound healing: Structural and functional prospects at biointerfaces. *Int J Bioprint*, 9(1): 648  
<https://doi.org/10.18063/ijb.v9i1.648>

**Received:** June 14, 2022

**Accepted:** August 29, 2022

**Published Online:** November 29, 2022

**Copyright:** © 2022 Author(s). This is an Open Access article distributed under the terms of the Creative Commons Attribution License, permitting distribution and reproduction in any medium, provided the original work is properly cited.

**Publisher's Note:** Whioce Publishing remains neutral with regard to jurisdictional claims in published maps and institutional affiliations.

## 1. Introduction

Blood loss associated with surgical procedures, trauma, or injuries can be lethal depending on the extremity of the damage<sup>[1]</sup>. Conventional hemostatic techniques, such as suturing or cotton gauzes, are inefficient in achieving rapid hemostasis. Therefore, developing efficient hemostatic platforms is crucial to advancing healthcare and medicine. Several hemostatic agents have been developed, including hemostatic powders, scaffolds, and patches, for patient care. Most hemostat were developed based on some of the standard guidelines to achieve perfect hemostat properties. These hemostat properties include rapid hemostasis, ready-to-use ability, user-friendliness, lightweight, and durability<sup>[2]</sup>.

Among the modern hemostats, multifunctional three-dimensional (3D) micro/nanohemostatic constructs have proven effective in numerous medical conditions,

like in cases where blood loss is associated with severe tissue damage<sup>[3]</sup>. Such severity often demands enormous tissue regeneration or repair following blood clots, which can be effectively managed by multifunctional 3D hemostats. Micro/nanostructure-enabled hemostat availability is favorable for clinical use because these novel agents have shown excellent inherent biomimetic properties following the body's natural wound healing process<sup>[4]</sup>. For instant, fabricating hemostatic agents capable of inducing angiogenesis, immune responses, and desired signaling pathways following blood clotting might serve as an effective hemostat<sup>[5-10]</sup>. Another reason why micro/nanostructured hemostatic agents have gained popularity is because of their ability to respond to intracellular and extracellular stimuli through their physical architecture<sup>[4]</sup>. Their architecture allows them to adapt quickly, closely connecting the structural and functional aspects of the biointerface. Additionally, when fabricating multifunctional 3D hemostats, characteristics such as desired topography, biocompatibility, mechanical stability, biodegradability, and antibacterial properties are fundamental properties under consideration, for which surface modification has shown excellent outcomes<sup>[11]</sup>. Because of this, choosing materials with biocompatible and anti-infection properties should be heavily considered when designing micro/nanostructures for rapid hemostasis. However, it is more advantageous to select materials and use fabrication techniques most appropriate to the needs of the individual based on the specific condition at hand<sup>[12-16]</sup>. Hence, innovation in the fabrication and use of 3D micro/nano-hemostats is necessary for improved medication.

Current technologies allow us to fabricate these structures via extrusion methods, electrospinning, soft lithography, stereolithography (SLA), digital light processing (DLP), 3D/4D printing, and combined methods to create hemostats with excellent biocompatibility, zero to low cytotoxicity, long-term stability, antibacterial activity, and among others<sup>[17]</sup>.

Thus, this paper aims to review the multifunctional 3D platforms, which are designed using advanced fabrication techniques, for rapid hemostasis and wound healing. It also aims to interpret the relevance of 3D micro/nanotopography in the functional prospect at the wound-implant interface. We anticipate this work will provide valuable information to develop future innovations concerning smart hemostats for biomedical applications.

## 2. Mechanism of wound healing and hemostasis

Each hemostat's mode of operation is determined by the degree of intrinsic variation in the material's physico-

chemical configuration, which regulates the natural course of the wound healing process. The natural wound healing process occurs in various overlapping stages, including hemostasis, inflammation, proliferation, and remodeling (Figure 1A). Each stage requires extensive communication between different cellular constituents of various compartments of the skin and its extracellular matrix (ECM)<sup>[18]</sup>, creating a dynamic and complex environment caused by the activation and influence of different signaling pathways of the coagulation cascade on each other. Interruption or deregulation of one or more overlapping phases may lead to non-healing (chronic) wounds in the wound healing process. Thus, the efficient design of functional micro/nanostructures to accelerate the physiological process of hemostasis is essential<sup>[19]</sup>; and elucidation of the body's natural hemostasis mechanisms, such as the natural blood coagulation cascade, is imperative for the fabrication of effective hemostatic agents<sup>[20]</sup>. The body's priority after an injury is to stop blood loss. The fibrin clot stops blood loss while trapping inflammatory cells like neutrophils, monocytes, macrophages, Langerhans cells, dermal dendritic cells, and T cells, among others<sup>[21,22]</sup>. The closure of the inflammatory phase follows the onset of angiogenesis, which involves endothelial cell proliferation, activation of pericytes, migration, and neo-blood vessel formation. While neo-angiogenesis prevails, fibroblasts proliferate and deposit ECM, indicating the growth stage of the healing tissue<sup>[23-29]</sup>. Re-epithelization occurs simultaneously, involving the proliferation of both unipotent epidermal stem cells and de-differentiation of terminally differentiated epidermal cells<sup>[30]</sup>. Re-epithelialization also involves the reconstruction of all skin appendages, including the formation of sebaceous glands, sweat glands, and hair follicles.

### 2.1. Cellular and molecular mechanisms of physiological hemostasis

Hemostasis marks the first stage of wound healing, including vasoconstriction, primary hemostasis, and secondary hemostasis. The key factor in hemostasis is the platelets, while the critical matrix component is the fibrinogen. A healthy endothelial cell monolayer in an unruptured blood vessel prevents the platelets' untimely activation, thereby preventing their adhesion to the vessel wall or clumping among each other. Vasoconstriction and formation of a fibrin clot in the bleeding site prevents blood loss after injury. The clot is formed from the adherence and aggregation of platelets. The generation of fibrin is then established from the activation of prothrombin to thrombin, where thrombin cleaves fibrinogen to form fibrin. A blood clot is followed by primary and secondary hemostasis. Primary hemostasis involves platelet aggregation and platelet plug formation

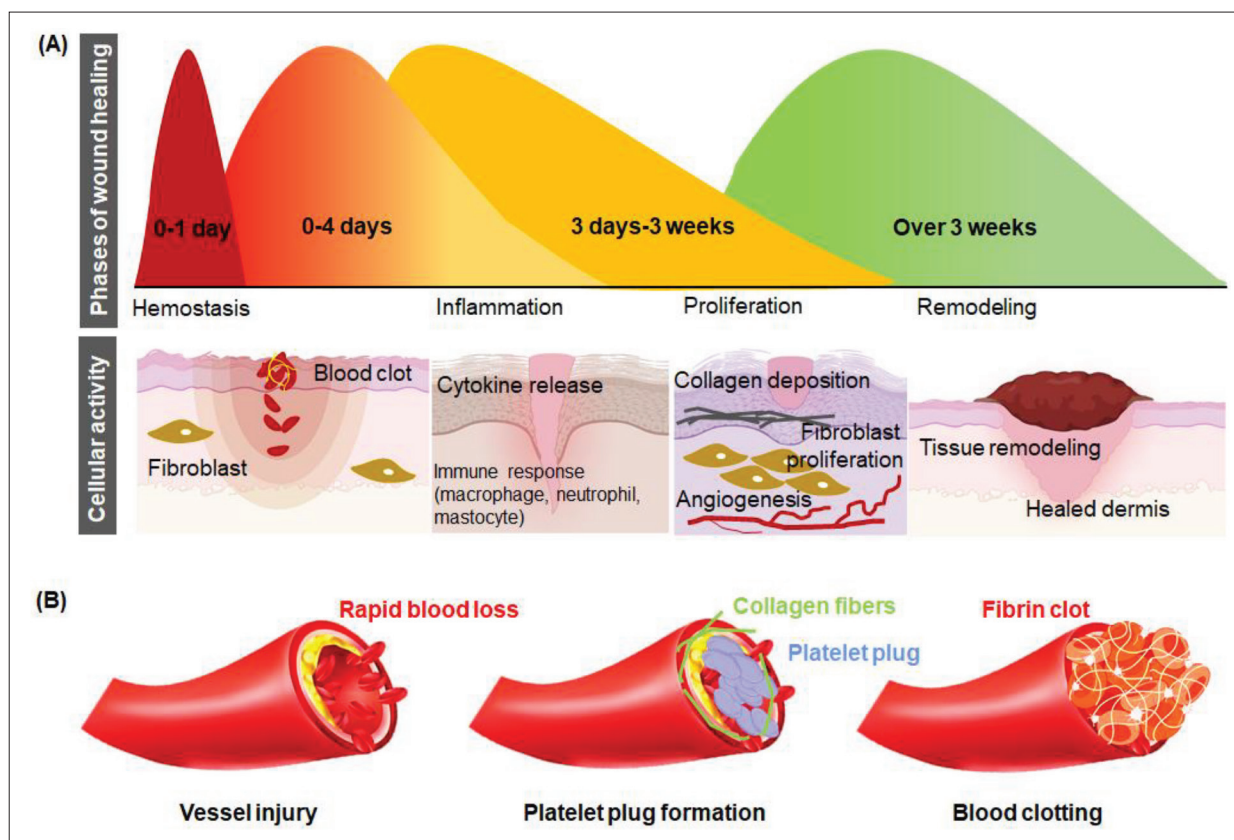


Figure 1. Schematic representation of (A) the stages of wound healing and (B) the hemostasis.

elicited by collagen exposure within the subendothelial matrix. The platelet plug and the fibrin mesh combine to form the thrombus, which stops bleeding and releases complement and growth factors, forming a template for successive wound healing<sup>[31]</sup>. Secondary hemostasis refers to the activation of the coagulation cascade where soluble fibrinogen is converted to insoluble strands that make up the fibrin mesh.

### 2.2. Vasoconstriction

Following injury, vasoconstrictors, such as endothelin, trigger the reflexive contracture of vascular smooth muscle, eventually reducing bleeding at the ruptured microvasculature. Besides, growth factors released from injured cells also promote vasoconstriction. These include catecholamine, epinephrine, norepinephrine, and prostaglandins. Growth factors like platelet-derived growth factors activate the mesenchymal cells, causing contraction. The initial reflexive constriction of the blood vessel might resume, resulting from local hypoxia and acidosis. The long-term clotting is thus realized by the downstream components of the coagulation cascade. This includes bradykinin, fibrinopeptide, serotonin, and thromboxane A<sub>2</sub><sup>[32]</sup>.

### 2.3. Primary hemostasis

Primary hemostasis is significantly regulated by the platelets, which are anucleate cells budding from megakaryocytes. The platelets circulate close to the endothelial cells. Following an injury, the thrombogenic subendothelial matrix is exposed. The exposed surface attracts the bonding of the platelets through their G-protein-coupled receptors. This activates the signal transduction cascade that causes integrin activation. Increased integrin activation leads to the platelets' attachment to other platelets and the surrounding ECM. The signal transduction cascade leads to the change in the conformation of actin filaments. Changes in the actin conformation transform the disk-shaped dispersed platelets into a round structure, eventually forming pseudopodia and lamellipodia. The formed appendages then attach firmly to ECM, mechanically sealing the blood vessel. Moreover, intracellular granules in platelets secrete numerous active substances, such as adenosine diphosphate, serotonin, calcium, and histamine, that are required for platelet activation and primary and secondary hemostasis<sup>[33]</sup>. The release of platelet factors is the most intense within the first hour of platelet activation, which can continue up to 7 days, resulting in a paracrine effect on other cell types, including smooth muscle cells, endothelial cells, monocytes, and fibroblasts<sup>[34,35]</sup>.

## 2.4. Secondary hemostasis

Platelets are the templates for the assembly and activation of coagulation complexes. The coagulation pathways involved usually is classified as intrinsic and extrinsic pathways. The exposure of the subendothelial matrix activates both the pathways, which leads to the activation of factor X. Following the activation of factor X, the prothrombin is converted to thrombin which cleaves fibrinogen to fibrin. Factor XIII then covalently crosslinks fibrin, which binds the aggregated platelet forming the secondary hemostasis, also known as the thrombus. The thrombus then serves as the wound matrix for infiltrating other cells until wound healing<sup>[36]</sup>. The various stages of wound healing and hemostasis are illustrated in [Figure 1B](#).

## 3. Structural and functional prospect of biomaterial at biointerface

Rapid promotion of hemostasis and subsequent biomimetic wound healing is possible via different micro/nanostructures<sup>[37,38]</sup>. These structures include nanotubes, nanofibers, and micro/nanoparticles. Although the hemostatic mechanism of nanotubes have not yet been fully elucidated, they have been utilized as hemostatic agents for thousands of years in traditional Chinese medicinal applications<sup>[39,40]</sup>. However, it has been recently discovered that nanotubes fabricated for rapid hemostasis have a high structural aspect ratio and surface area. Owing to this, hemostasis proceeds via plasma or fluid interaction through one of these mechanisms: (i) efficient water absorption, leading to material concentration; (ii) factor XII activation within the intrinsic coagulation cascade, which in turn causes ionic bonding of amino acids; or (iii) the formation of a physical barrier that stops further hemorrhage. The mechanism of hemostasis varies depending on the structural aspect associated with the type of materials used in their fabrication, but micro- and nanofibers tend to operate through a similar mechanism. Molecules are self-assembled into a micro/nanofiber mat-like structure, leading to improved platelet binding. This micro/nanofiber mat promotes blood clot formation by accelerating fibrin, platelet, and red blood cell (RBC) coagulation on the material's surface. Micro/nanoparticles, including micro/nanospheres and adhesive powders/gels, are small and feature a high surface area. Although the molecular mechanism for micro/nanoparticles is not yet well understood, we can confirm that there is a promotion of blood cell and platelet aggregation on the surface of the micro/nanostructures due to physical factors of incurred water absorption and consequent swelling. Some micro/nanoparticles induce rapid hemostasis through liquid absorption in the formation of an *in situ* hydrogel. This absorption leads to the concentration of blood cells,

platelets, and other coagulation factors, thus creating a physical barrier to stop further hemorrhage. Due to the inherent dynamic properties of all micro/nanostructures, both can create a suitable 3D microenvironment to support cell activities, such as adhesion, growth, and differentiation, for biomimetic wound healing and effective hemostasis modulation<sup>[41,42]</sup>. Some unique micro/nanostructures and their hemostatic mechanisms are summarized in [Table 1](#).

Therefore, to effectively represent the spatiotemporal functionality of the target tissue's dynamic environment, micro/nanostructure design for hemostasis requires a conscientious selection of fabrication materials and close attention to its architectural constitution in addition to the inherent physical and biochemical properties<sup>[43]</sup>.

### 3.1. Structural modulation

The micro/nanostructures in hemostats accelerate the onset of hemostasis through multiple mechanisms, including rapid blood absorption, faster blood clot formation, and altered cell dynamics and behavior<sup>[44,45]</sup>. Microproperties of a hemostatic agent can be tuned depending on the manufacturing technique used to shape the materials used for its fabrication. For example, cell anchorage is a defining characteristic that can be tuned in scaffolds for hemostasis via microstructures. This tunability is crucial to hemostat functionality because cell anchorage to the scaffolds via microstructure interaction can promote cell adhesion, facilitating the mediation of cell morphology and subsequent differentiation. For example, topographical features such as pillar height have proven relevant in affecting traction and reaction force upon cells when subject to lateral displacement, which directly affects cellular attachment and subsequent behavior ([Figure 2A](#)). Physical properties, such as stiffness and elasticity, have also been proven to affect cell morphology by altering the cytoskeletal organization and contractibility, guiding stem cell differentiation into specific lineages<sup>[46]</sup>.

#### 3.1.1. Microscale structures

Polymeric microstructures with rough and random pores (~5–10  $\mu\text{m}$ ) are promising topological attributes that facilitate interfacial interaction between RBC and the hemostat leading to rapid RBC aggregation ([Figure 2B](#)). These microstructures often act as molecular sieves that absorb water in the blood and concentrate RBC promptly<sup>[47,48]</sup>. Microscale structures are also favored in the fabrication of on-demand hemostatic microbots. The micropatterns in the hemostat are often loaded with drug materials to make them effective drug delivery vehicles for rapid blood clotting. Furthermore, the microstructure pattern mediates drug delivery for hemostasis spatiotemporally with stimuli-responsive materials. These microstructure-oriented systems can be controlled via



Table 1. Structural properties of fabricated micro/nanostructures in hemostatic applications

Hemostat fabrication process	Type of micro/nanostructure	Structural properties	Mechanism of hemostasis	References
3D/4D printing, electrospinning, extrusion methods, stereolithography	Nanotube	High structural aspect ratio	<ul style="list-style-type: none"> <li>• Plasma interaction</li> </ul>	[155]
		High surface area	<ul style="list-style-type: none"> <li>• Plasma interaction</li> <li>• Fluid adsorption</li> </ul>	[39,61,156]
3D/4D printing, electrospinning, soft lithography	Micro/nanofiber	Small diameter	<ul style="list-style-type: none"> <li>• Physical mesh-like hemostatic barrier</li> <li>• Platelet interaction</li> <li>• Plasma interaction</li> </ul>	[157-160]
		High structural aspect ratio	<ul style="list-style-type: none"> <li>• Platelet entrapment</li> <li>• Red blood cell entrapment</li> <li>• Blood component entrapment</li> <li>• Mechanical strength inhibits blood loss</li> <li>• Platelet adhesion</li> </ul>	[7,60,90,161-164]
		High surface area	<ul style="list-style-type: none"> <li>• Drug delivery agent</li> <li>• Platelet adsorption</li> <li>• Plasma adsorption</li> <li>• Red blood cell adsorption</li> <li>• Fluid adsorption</li> <li>• Intrinsic pathway activation promotes plasma coagulation</li> </ul>	[7,37,161-163,165-167]
3D/4D printing, electrospinning, digital light processing	Micro/nanoparticle, Micro/nanosphere, Adhesive powder/gel	Small size	<ul style="list-style-type: none"> <li>• Drug delivery agent</li> <li>• Tissue adhesion</li> <li>• Platelet adsorption</li> <li>• Plasma adsorption</li> </ul>	[140,168-171]
		High surface area	<ul style="list-style-type: none"> <li>• Drug delivery agent</li> <li>• Platelet adsorption</li> <li>• Plasma adsorption</li> <li>• Plasma coagulation</li> <li>• Red blood cell adsorption</li> <li>• Ion-induced platelet activation</li> </ul>	[131,172-175]

user-defined release kinetics using temperature, pH, and light stimuli, among others<sup>[47,49]</sup>. Some popular release systems for this purpose include the programmed delivery of one or multiple compounds necessary to promote rapid hemostasis, such as fibrinogen and thrombin<sup>[50]</sup>.

Coagulation experiments have determined that composite microparticles can both reduce the bleeding time and accelerate coagulation rates, in addition to having the ability to be used in combination with hemostatic adhesive powders/gels, such as chitosan-based composites<sup>[41]</sup>. Microparticles inlaid in scaffolds allow for targeted delivery of erythrocytes to decrease clotting time<sup>[51]</sup>. Microspheres with morphologically relevant surface structures, such as “macropits” or “craters,” enhance hemostasis by promoting fluid absorption. The increased fluid absorption rate and ratio both incur rapid hemostasis and subsequently decrease the size of the wound area<sup>[52]</sup>. In addition, the surface roughness of microscale structures is proportional to faster coagulation rates and increased strength due to

the promotion of blood cell aggregation that this surface roughness permits<sup>[17,53]</sup>. Microspheres can also strengthen the hemostat’s intrinsic properties, allowing rapid blood clot formation and enhanced adhesion to cells and tissue<sup>[54-56]</sup>. Adhesive microgels are powdered microstructures and feature a high surface area. They induce rapid hemostasis through liquid absorption, forming an *in situ* hydrogel. These microgels lead to the concentration of blood cells, platelets, and other coagulation factors, thus creating a physical barrier to stop further hemorrhage<sup>[57]</sup>.

### 3.1.2. Nanoscale structures

At the nanoscale level, surface biochemistry instructs cell behavior by directly mediating the cell–material interactions or initiating surface receptor activation. Nanostructures function as mediators in modulating biochemical cues, such as activating growth factors and proteins. Additionally, these nanostructures can alter communication between cells and the fabricated scaffold to induce a more rapid biochemically activated

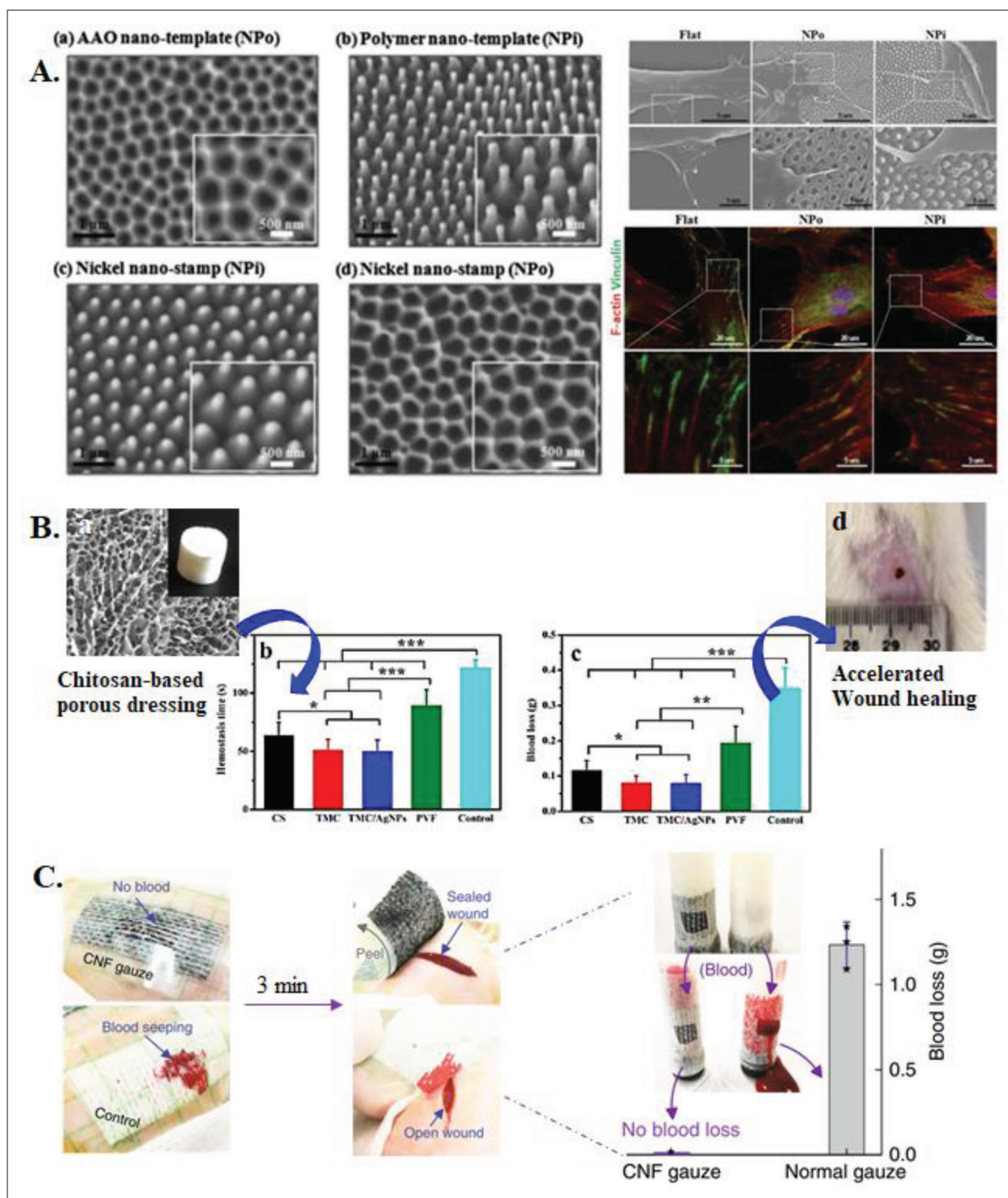


**Figure 2.** Effects of structural modulation on cell behavior and response. (A) Micropillar arrays of different diameters and morphologies affecting cell adhesion and actin orientation<sup>[6,141]</sup>. (B) Chitosan-based porous wound dressing with excellent hemostatic properties<sup>[51]</sup>. (C) Hemostatic evaluation of a CNF gauze<sup>[37]</sup>.

hemostatic response<sup>[58]</sup>. Nanotopographical cues are among the most critical factors which help to mediate cell adhesion, mainly through the interactions between proteins and ECM<sup>[18]</sup>. Thus, controlling these interactions via topographical features can synergistically improve cell

behavior. One example of the topographic modifications on the nanoscopic scale comes from a study by Nouri-Goushki et al.<sup>[6]</sup>. This study revealed that the design of specific 3D-printed surface-modified surface grooves and nanopatterns directly affects cell adhesion forces,

cytocompatibility, cell adhesion, morphology, elastic modulus, and the subsequent cell behavior<sup>[56]</sup>.

Nanofibers are often fabricated to make composite mats that activate intrinsic and extrinsic coagulation pathways, thus entrapping blood cells and platelets through a physiological mechanism. They can also be promoters of self-assembling peptides in forming a physical barrier to reduce hemorrhage through a physical mechanism<sup>[59,60]</sup>. Recent studies have incorporated carbon nanofibers (CNFs) into gauzes to promote hemostasis. When these plaster-like gauzes patch onto incisions on a rat's back, the control cotton gauze gets wet quickly, while the CNF gauze prevents blood loss. Three minutes later, the CNF gauze helps form a gel-like clot, properly sealing the wound, while an open wound remains under the control gauze (Figure 2C).

Nanotubes exhibit a hollow tubular structure, making them easy to immobilize on polymeric matrices like chitosan or cellulose. This property further adds to their biocompatibility and hemostasis through an extensive hydrogen-bonding network for improved functionality<sup>[61]</sup>. Nanospheres are yet other nanostructures for hemostasis because of their ability to self-assemble, form ionic crosslinking interactions, and self-emulsify to form a uniform barrier without surfactants<sup>[62]</sup>. Apart from exhibiting properties of high biocompatibility, novel hollow nanospheres have proven to be excellent carriers of antibacterial agents for biomimetic nanozyme-based wound healing<sup>[49]</sup>.

### 3.1.3. Active materials

There has been increased development in the search of hemostatic materials for novel micro/nanostructure design, especially in maximizing the potential of their inherent physicochemical properties<sup>[63-65]</sup>. Various active hemostatic materials have helped optimize the design and fabrication of different micro/nanostructures for rapid hemostasis. Such active materials include natural and synthetic polymers. Natural polymers all have favorable biocompatibility, bioactivity, degradability, and viscoelasticity, and they can be easily processed, and are able to resemble the ECM of native tissues<sup>[7]</sup>. However, the disadvantages of natural polymers typically include low mechanical strength, chemical instability *in situ*, and high cost, among others. Synthetic polymers include artificial materials, such as polyethylene glycol, polyvinyl alcohol, and polyurethane. We have seen an increase in the use of these materials due to their ability to avoid the drawbacks posed by natural polymers. Synthetic polymers include artificial materials, such as polyethylene glycol, polyvinyl alcohol, and polyurethane. These materials have increased in use due to their ability to avoid the drawbacks of natural

polymers. However, they still have the limitations of slow biodegradation and high cost. Inorganic materials have significant hemostatic effects, but they have also exhibited potential metabolic toxicity.

Nevertheless, inorganic materials coupled with metals as composites exhibit enhanced hemostatic potential. These metals include calcium, silver, gold, zinc, iron, and cerium<sup>[19,41,49]</sup>. The enhanced hemostatic potential enables the effects of active materials on the functional and biological modulation of hemostasis.

### 3.2. Functional modulation

Functionalized materials has a significantly high potential in regulating the events of the coagulation cascade<sup>[19,37]</sup>. The following examples as shown in Table 2 highlight current clinical applications of such materials in micro/nanostructure development, while the examples in Table 3 outline favorable characteristics of materials with inherent hemostatic properties in novel micro/nanostructure development for rapid hemostasis.

Although different materials stimulate hemostasis and subsequent wound healing through various mechanisms, they often operate in different *in vitro* and *in vivo* settings due to the dynamic nature of the ECM *in vivo* conditions<sup>[45,66]</sup>. Additionally, the morphology of selected materials is one of the main factors determining the resulting hemostat's functional properties, thereby directly affecting subsequent micro/nanostructure-mediated bioactive behaviors<sup>[16]</sup>. For example, the fibrous morphology of proteins such as collagen, elastin, and fibrin allow for anisotropy of the ECM, promoting cell migration, proliferation, and differentiation. Bone tissues made from fibrous protein matrices are a practical reference. Another reference to the importance of morphology is cell alignment in muscle cells, which bestows these tissues their tensile strength<sup>[67]</sup>. Materials commonly used to rebuild natural ECM-like conditions include hyaluronic acid, polyacrylamide, polyethylene glycol, and poly L-lactide combined with natural compounds, such as collagen, fibrin, and peptide amphiphiles<sup>[44]</sup>. We can further utilize these materials when designing micro/nanostructures to support their biomimetic and hemostatic capabilities further. For example, self-assembling peptide nanofibers have the spatiotemporal abilities to incur rapid hemostasis through the promotion of platelet concentration, thereby accelerating the coagulation cascade through physical modulation and surface patterning<sup>[60,68,69]</sup>.

### 3.3. Biological modulation

Inlaid micro- and nanoscopic surface patterns and hemostatic agents respond to the body's biochemical and mechanosensory signals via active biomolecules

**Table 2. Biomaterial-oriented clinical applications in micro/nanostructure development**

Biomaterial	Major clinical applications	References
<i>Synthetic degradable polyesters</i>		
Poly(lactic acid) (PLA), poly(glycolic acid) (PGA)	Sutures	[176,177]
Poly(hydroxybutyrate) (PHB), Poly(hydroxyvalerate) (PHV)	Long-term drug delivery; artificial skin; surgical patching materials	[178,179]
<i>Synthetic degradable thermoplastic polymers</i>		
Polyester, PVC	Drug delivery; adhesives	[180-182]
<i>Natural resorbable polymers</i>		
Collagen	Drug delivery; blood contacting devices	[183,184]
Fibrinogen, fibrin	Drug delivery; gene delivery; artificial skin; coating to improve cellular adhesion; soft tissue augmentation; scaffold for blood vessel reconstruction; wound closure; hemostatic agent	[185-187]
Hyaluronic acid	Tissue sealant; cell delivery	[186,188-190]
<i>Natural resorbable polysaccharides</i>		
Cellulose	Drug delivery; wound dressing applications	[191-193]
Chitosan	Adhesion barrier; hemostat	[194-198]
Alginate	Hydrogel; wound dressing applications	[53,55,199]
Gelatin	Hydrogel; hemostat; wound dressing applications	[7,124,200]
Elastin	Hemorrhage impedant	[201-203]
Heparin	Surgical mesh	[204-206]
<i>Metals and alloys</i>		
Silver	Antibacterial agents	[131,140,168]
Platinum, platinum-iridium	Electrodes	[207-209]

and mediators. Active biomolecules include immune response mediators and growth factors, while mediators include factors that affect stimulus responsivity, mechanotransduction, and biophysical interactions. Thus, incorporating micro/nanostructures releases these active biomolecules for the proper cellular function throughout the wound healing process.

Through current advances in elucidation of material properties, we can see that there has been improved micro/nanostructure functionality as hemostatic agents, including the incorporation of various immune response mediators in their design. These immune response mediators promote cell differentiation and direct macrophage differentiation to pro- and anti-inflammatory phenotypes<sup>[70,71]</sup>.

Hemostatic agents incorporating micro/nanostructures and immune response mediators can ensure a rapid hemostasis promotion at the onset of application with subsequent strong clot adhesion on the material application site through promoting cell adhesion<sup>[63-65]</sup>.

These factors mentioned above can also be applied to developing and applying a sequential drug delivery system for bioactive factors during hemostasis and wound healing using the inherent properties of micro/nanostructures<sup>[72,73]</sup>. Hydrogels incorporated with micro/nanostructures

are used to assist in the on-demand delivery of drugs in the form of small molecules, proteins, and various nanoparticles<sup>[74,75]</sup>.

Recent research has focused on elucidating the effect of implanting micro/nanostructures laden with growth factors into composite/hybrid biodegradable hydrogels and scaffolds. Studies have found that the responsivity of micro/nanostructures creates a biomimetic effect similar to the ECM in these fabricated hemostatic agents, providing a secure means to manipulate a hemostat's bioactive properties. Rapid hemostasis in diabetic wounds has been achieved by incorporating growth factors including epidermal growth factor, transforming growth factor-beta, fibroblast growth factor, vascular endothelial growth factor, and platelet-derived growth factor<sup>[45,76-78]</sup>. The controlled release of various growth factors and other cellular components has also played a significant role in tissue regeneration through their release and activation at various phases of the wound healing process. Thrombin generation has also been shown to be possible when laden onto polyphosphate-crosslinked collagen scaffolds.

Controlled release via micro/nanostructures' stimulus responsivity is significant to hemostasis and wound healing because stimuli external to the ECM, such as



**Table 3. Biomaterials for fabricating micro/nanostructures as hemostatic agents**

Hemostatic material	Hemostatic mechanism	Role in wound healing	Limiting factors	References
<i>Synthetic polymers</i>				
Polyethylene glycol (PEG)	Tissue adhesion	Carrier for therapeutic agents	Expensive; risk of residue	[64,210,211]
Polyurethane	Platelet aggregation; coagulation initiator	Antibacterial agent	Slow biodegradation; poor biocompatibility; long polymerization time	[212-214]
<i>Natural polymers</i>				
Collagen and gelatin	Platelet activation	Promotes cell growth and proliferation	Poor resistance to degradation; risk of immune response	[7,124,183,184,200]
Fibrinogen, fibrin	Blood clot formation; platelet aggregation	Revascularization; promotes epidermal thickness; promotes fibroblast and fibrocyte proliferation	Expensive; risk of immune response	[185-187]
Hyaluronic acid	Tissue adhesion	Wound moisture; promotes fibroblast migration and collagen deposition	Expensive; difficult to remove	[186,188-190]
Cellulose	Platelet aggregation; coagulation factor activation	Antibacterial agent	Slow biodegradation	[191-193]
Chitosan	Platelet and blood cell adhesion and aggregation	Antibacterial agent; promotes granulation tissue formation; promotes fibroblast proliferation	Poor biocompatibility; slow degradation	[194-198]
Alginate	Tissue adhesion	Wound moisture; promotes tissue granulation and fibroblast proliferation	Low mechanical strength and chemical stability	[53,55,199]
Curcumin	Immuno-regulator	Antibacterial agent; anti-inflammatory; antioxidant; anti-carcinogenic	Poor bioavailability and absorption; chemical instability	[215-218]
<i>Metal-containing materials</i>				
Silver (Ag)	Platelet activation	Antibacterial agent	No biodegradation; difficult to remove; toxic at high concentrations	[68,219-222]
Zinc (Zn)	Blood cell aggregation	Antibacterial agent; epithelization; revascularization; promotes cell proliferation		[68,174,190,216]
Iron (Fe)	Blood cell aggregation; thrombin stabilizer	Revascularization		[40,68,171,215,219]
Cerium (Ce)	Blood cell aggregation	Anti-inflammatory		[223-225]
Gold (Au)	Phagocytosis	Enzymatic activity modulation, anti-carcinogen		[226-228]

electrical, light, and ultrasound stimulations, play a role in determining stem cell behavior<sup>[44,74]</sup>. Topographical modifications can modulate monocyte attachment and macrophage differentiation. Figure 3A shows the polarization of naïve (M0) macrophages to pro- (M1) or anti-inflammatory (M2) phenotypes. Electrification at different power densities for a sustained amount of time is also an effective means of killing bacteria<sup>[70]</sup>. For example, Figure 3B shows the bacterial killing rate in a topical wound dressing as a function of the time of white light irradiation (400–800 nm) at different power densities<sup>[71]</sup>.

Micro/nanostructures also have an inherent ability to respond to stimuli, such as temperature, and translate these cues to create a more dynamic 3D microenvironment. Thus, photothermal and photodynamic therapy has been utilized to initiate the onset of more rapid hemostasis and support

subsequent wound healing in hydrogels infused with micro/nanostructures. Figure 3C shows the comparative effects in hemostasis and subsequent wound healing between a hemostatic agent made of quaternized chitosan, a hydrogel, and a hydrogel infused with near-infrared (NIR)-responsive micro/nanostructures<sup>[79]</sup>. These examples show the significance of utilizing materials that allow for a more fine-tuned response to stimuli in micro/nanostructures when designing scaffolds seeded with growth factors and cells that require controlled activation<sup>[45]</sup>.

#### 4. Micro/nanostructures in hemostatic application

Appropriate material selection and fabrication techniques are necessary for designing and fabricating scaffolds and micro/nanostructures for rapid hemostasis. When

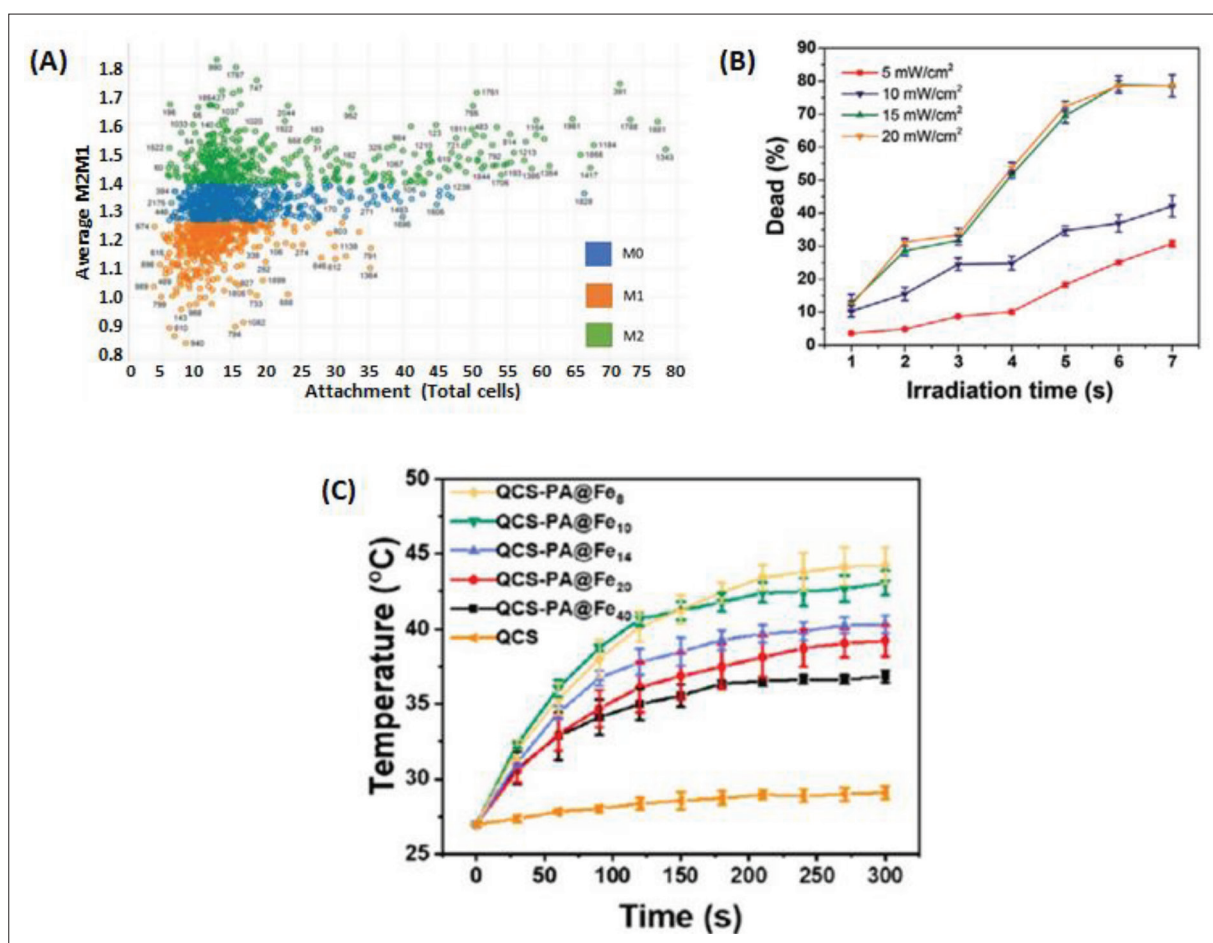


**Figure 3.** Effect of biological modulation on hemostatic properties of micro/nanostructures. (A) Scatter plot of Topo Unit phenotype (average M2/M1 ratio) and macrophage attachment<sup>[70]</sup>. (B) Bacterial killing rate via white light irradiation (400–800 nm) at power densities 5, 10, 15, and 20 mW/cm<sup>2</sup><sup>[71]</sup>. (C) Graph and photographs of temperature enhancement and NIR irradiation on hydrogels<sup>[79]</sup>.

we combine materials with a specified fabrication technique, we can easily manipulate aspects such as the hemostat's final macroscopic structure, mechanical properties, and biological responses. To date, there have been many accomplishments regarding scaffold and micro/nanostructure fabrication techniques due to the development and widespread use of novel technologies<sup>[80,81]</sup>. In addition, current scaffold and micro/nanostructure fabrication techniques, such as electrospinning, freeze-drying, bioprinting, and decellularization, have been proven to be effective strategies to create hemostats that improve vascularization potential and immunomodulation for a more biomimetic healing process<sup>[38,58,82]</sup>.

#### 4.1. Electrospinning

Electrospinning has seen an increase in application for hemostat development since the early 2000s. These techniques have many applications across various fields, mainly due to the inherent properties of scalability and versatility that electrospinning offers for designing

novel hemostats. For instance, this approach has been effectively applied to biosensing, drug delivery, soft and complex tissue regeneration, and the fabrication of various micro/nanostructures for hemostasis and wound healing applications. Electrospinning allows for much control over factors, such as fiber geometrical characteristics, alignment, and architecture. In addition, the materials used in the electrospinning and manufacturing processes influence a nanofiber's level of control in the modulation of cell behaviors. Precise control in manufacture is beneficial for applying micro/nanostructures in hemostat development, as electrospun nanofibers play a vital role in manipulating cell behavior via the efficient promotion of cell adhesion, proliferation, and differentiation through the high tunability of properties at the nanoscale<sup>[44]</sup>.

One example of a highly effective micro/nanostructure-enabled hemostatic agent is the electrospun ultralight 3D gelatin sponge consisting of continuously interconnected nanofibers designed by Xie et al.<sup>[7]</sup>. Owing to this nanofiber

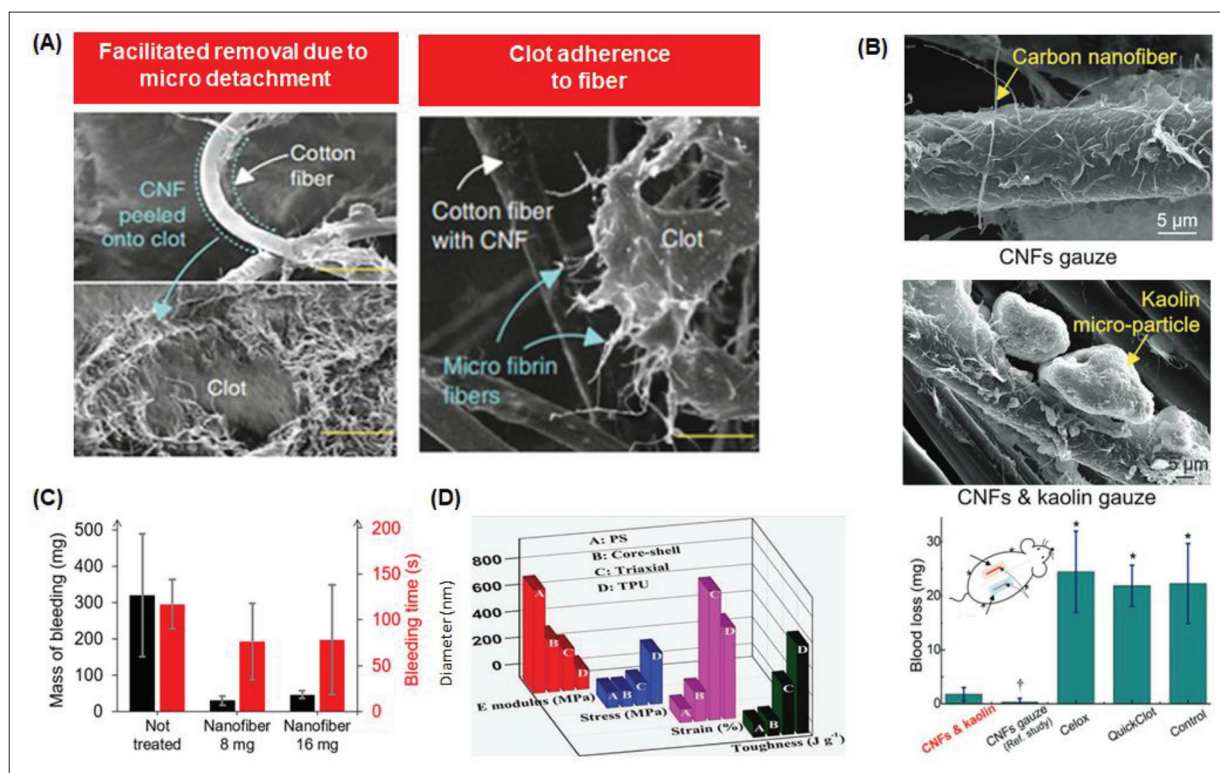


**Figure 4.** Electrospun micro/nanosurfaces for rapid hemostasis. (A) Scanning electron microscopy (SEM) image of microfibrin fibers adhered on CNFs-coated cotton fibers after clot shrinkage<sup>[37]</sup>. (B) Blood loss of hemostatic gauzes<sup>[83]</sup>. (C) Effect of nanofiber weight on mass and the time of bleeding<sup>[152]</sup>. (D) Effects of fiber diameter on mechanical properties<sup>[91]</sup>.

structure, the sponge has low density, high surface area, and compressibility potential, and feature an ultra-strong liquid absorption capacity. *In vitro* assessments confirmed the good cytocompatibility and biodegradability of the fabricated hemostatic sponge, as well as its ability to accelerate the formation of platelet embolism while activating both the intrinsic and extrinsic coagulation pathways in its mechanism of hemostasis. Further *in vivo* assessments demonstrated the gelatin nanofiber sponge's ability to rapidly induce stabilization of blood clots, thereby leading to the least amount of blood loss compared to other commercialized products currently in use, thus proving its advantage as a hemostatic agent<sup>[7]</sup>. Other studies on nanofiber composites have also demonstrated the ability of these structures to promote rapid hemostasis and incur minimal secondary damage due to the composites' intrinsic property of super-hydrophobicity and high user tunability<sup>[37,83]</sup>.

Electrospun fibers allow nanoscopic-level control over factors, such as fiber surface modifications and architecture<sup>[84,85]</sup>. Along with material choice, this control allows for tunability of the desired effect, such as hemostatic capacity and adherence strength. For example, Figure 4A shows a study by Li et al.<sup>[37]</sup>, which described

the development of a CNF-coated cotton fiber gauze for facile dressing removal after clot shrinkage. CNFs were transferred onto the clot after facile detachment, resulting in smooth cotton fiber and a hairy clot surface. Results indicated that the CNF gauze helps form a gel-like clot that properly seals wounds, while an open wound remains under any control gauze.

Electrospinning techniques are also widely used and valued for their submicron precision in fabrication in the design of various hemostatic agents<sup>[67]</sup>. Submicron precision in design is necessary because tunable factors, such as morphology, mechanical, electrical, and magnetic stimulations, influence the type and extent of cell-substrate interactions in micro/nanostructures<sup>[74]</sup>. Therefore, electrospinning techniques can be used as a micro/nanostructure fabrication method, which is a biomimetic approach to hemostasis and wound healing to inhibit undesirable side effects optimally<sup>[45]</sup>.

To this end, CNFs are used extensively because of their conductive properties<sup>[14,86-88]</sup>. Furthermore, incorporating CNFs into hydrogels allows for a biomimetic, electrically conductive environment that provides a platform for further development of controlled drug release and



increased antibacterial activity<sup>[89]</sup>. Platelets adhesion to nanofibers also becomes possible, as does fiber weight loss due to changes in pH throughout the wound healing process. Such CNF-enabled wound dressings show promise for synergistic therapy involving NIR-responsivity via photodynamic chemotherapy for hemostasis and subsequent wound healing. Aside from conductivity, these wound dressings feature the beneficial properties of biocompatibility and shape adaptability, all of which allow for the maintenance of a bioactive and controllable microenvironment<sup>[49,90]</sup>.

For example, in [Figure 4B](#), blood loss is evaluated for the prepared nonwetting CNF–kaolin composite nanostructured wound dressing measured at 5 minutes compared to the CNF gauze from a reference study<sup>[83]</sup>. This study used the commercial fast clotting gauzes (Celox and QuickClot) and the standard gauze (control).

Other studies<sup>[74,91]</sup> have revealed that fiber weight affects a hemostat's time to achieve hemostasis ([Figure 4C](#)). Similar studies have shown that fiber diameter affects resultant mechanical properties such as Young's modulus, stress, strain, and toughness ([Figure 4D](#)). Through this tunability and other features, such as low density and high porosity, multifunctional electrospun aerogel fibers have attracted much attention lately as a novel platform for hemostat design<sup>[92–94]</sup>. Along with excellent mechanical properties and increased surface area, conscientious material selection allows aerogel fibers the properties of superhydrophobicity and excellent thermal insulation performance, thus allowing them to be ideal candidates for hemostat development<sup>[95]</sup>.

#### 4.2. 3D printing

Even though we highly value electrospinning techniques for manufacturing effective hemostatic agents, it is not the only technique applied in hemostat design. Additive manufacturing techniques, such as 3D printing, have favorable results in fabricating various hemostatic agents, particularly those incorporating micro/nanostructures into their design. These hemostatic agents promote hemostasis and support wound healing utilizing topically administered methods, intracavitary, or intravenous applications. Popular 3D-printed hemostatic agents include gels, adhesives, sealants, patches, sponges, scaffolds, and foam-creation products. We favor porous agents, such as scaffolds and hydrogels, because of their ability to disrupt scar formation via their architecture<sup>[85,96]</sup>. Chitosan–PLA composites are highly favored materials for 3D printing because of their ease in printing micro/nanosurfaces ([Figure 5A](#)). Fabricated hemostatic agents can facilitate cell attachment, promoting tissue regeneration through printed micro/nanostructures and surface patterning.

Due to inherent fabrication properties, such as incurred stress and adhesion levels, the hemostatic agents may induce different hemostasis mechanisms. Such mechanisms proceed either by mechanical promotion, augmentation of the blood clotting cascade, binding tissues or blood vessels via adhesion kinetics, or preventing leakage from blood vessels<sup>[66]</sup>. However, all resultant 3D-printed hemostatic agents feature properties beneficial to rapid hemostasis, such as porosity, immunomodulation, and a pro-coagulant effect based on material selection<sup>[77,97]</sup>.

Cryogenic 3D-printed hydrogel scaffolds are one type of hemostatic agent currently manufactured for rapid hemostasis and subsequent diabetic and chronic wound healing support. Other hemostats include porous Ga-MBG/CHT composite scaffolds of various sizes fabricated via the interaction of NH<sub>2</sub> and OH groups of CHT with silanol groups of Ga-MBG.

3D printing of hemostatic agents allows the resulting construct to undergo a series of macroscopic compression and expansion, with little to no incurred damage. The sponge's original morphology can be quickly restored after being subject to varying degrees of compression<sup>[98]</sup>. Similarly, several studies demonstrate the compression stress–strain curves of freeze-dried 3D-printed honeycomb structures with cellulose concentrations of 4, 5, and 6 wt%<sup>[99]</sup>.

By incorporating micro/nanostructures, such as micro/nanoparticles, into the fabricated scaffold dressing, promoting hemostasis in these hydrogels becomes possible through the release of bioactive exosomes and the sustained proliferation and migration of cells<sup>[100]</sup>. 3D printing also affects the blood clotting kinetics of composite scaffolds, as shown in [Figure 5B](#).

Another hemostatic agent developed using 3D printing technologies is scaffolds combined with hybrid hydrogels laden with microparticles of chitosan methacrylate (CHMA) and polyvinyl alcohol (PVA). This material combination allows for the fabricated scaffold's mechanical properties tunability, thus imbuing the resulting agent with the most optimal viscoelasticity and shear thinning characteristics for spatiotemporal manipulation to ensure rapid hemostasis. A CHMA–PVA mixture also supports the growth of cells. It provides the inlaid microparticles with the necessary responsivity to differentiate these cells via the spatiotemporal translation of chemical, physical, and bioactive cues throughout the wound healing process<sup>[101]</sup>.

Using biodegradable 3D-printed polyurethane hydrogel–scaffold composites (G-DLPU3) also helps induce hemostasis and reduce the wounded area over time<sup>[102]</sup>. Adhesion kinetics of hemostatic glues, such as cyanoacrylate (CA) and other rigid adhesives (TA),



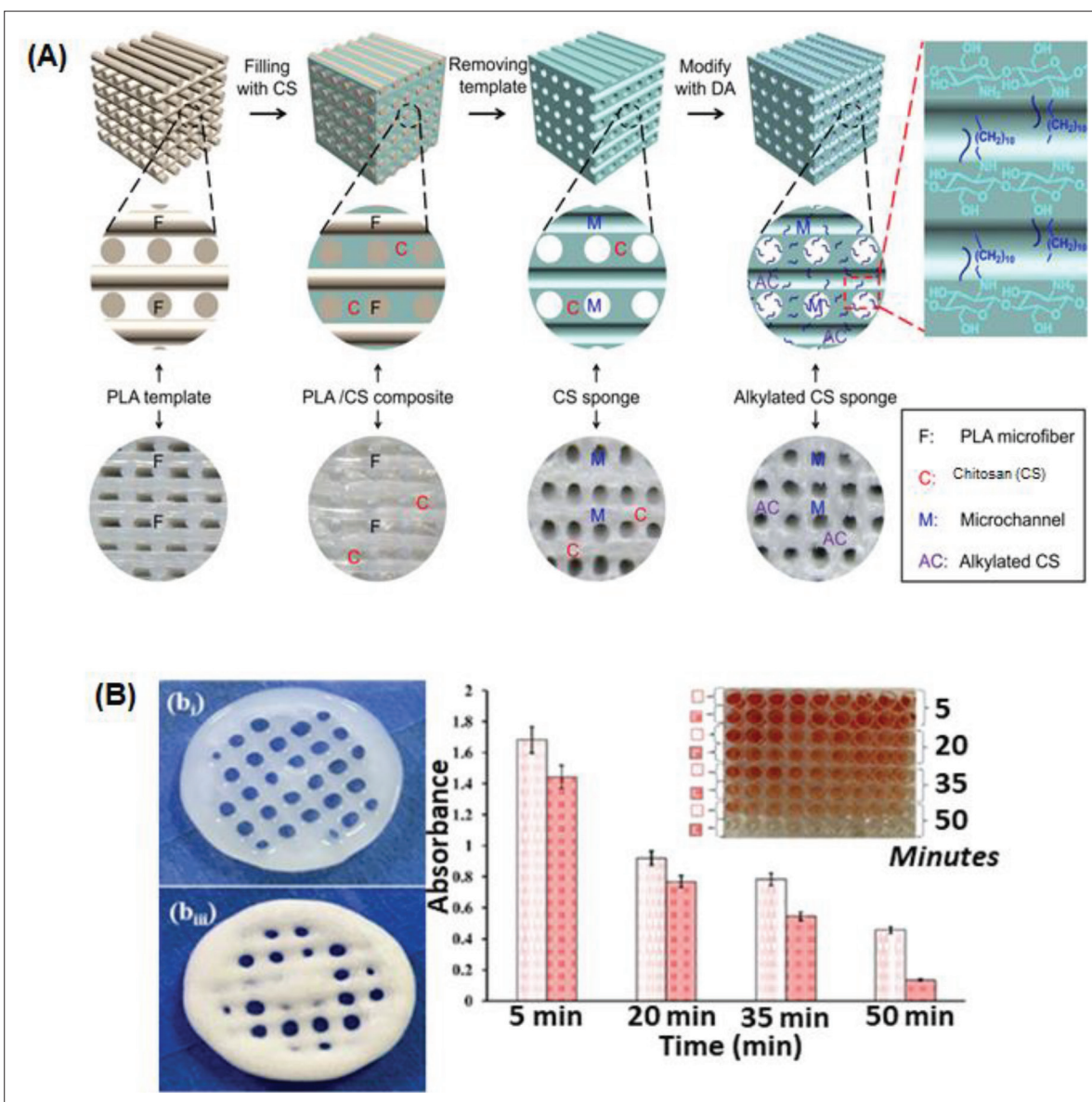


**Figure 5.** 3D/4D printing of micro/nanosurfaces for rapid hemostasis. (A) Schematic illustrations of 3D/4D-printed micro/nanosurfaces using PLA and chitosan<sup>[3]</sup>. (B) Blood clotting kinetics at different times<sup>[153]</sup>.

strengthen over time when exposed to blood. These inherent properties of hydrogels allow for a more rapid hemostasis when combined with 3D-printed scaffolds laden with micro/nanosurface modifications<sup>[103]</sup>.

3D printing offers a scaffold-free approach to developing artificial human skin patches for hemostasis and wound healing applications<sup>[104]</sup>. Chitosan-based inks are primarily used for this method of tissue regeneration. This is because chitosan-based solutions support cell proliferation and differentiation and allow for tunability and mimicry of the ECM. Because of the structure and composition of chitosan, slow gelation

rates and weak mechanical strength are drawbacks to using this natural polymer in a scaffold-free hemostatic approach. However, chitosan-based materials can be coupled with other materials to improve the possibility of a more substantial crosslinking and increase mechanical strength<sup>[105]</sup>.

In addition to 3D printing technologies, recent years have seen the advancement of 4D printing, which adds multidimensionality through time-sensitive interventions via material selection<sup>[50]</sup>. We can utilize programmed therapeutics to assist the body's natural regenerative responses in combined printing techniques<sup>[7]</sup>.

### 4.3. Combined techniques

Current technological advancements have allowed experts in the field of tissue engineering to expand the applicative range of various micro/nanostructure-hydrogel constructs to a much more comprehensive range of applications. This rapid expansion in applications has mainly been possible due to the breakthrough discovery involving the design of stimuli-responsive nanocomposite hydrogels, which biomimetically respond to internal and external biophysical and biochemical stimuli from the macroscopic to the nanoscopic scale<sup>[106]</sup>. Thus, additive manufacturing and electrospinning techniques are currently the potent and practical tools for tissue engineering applications, especially in manufacturing micro/nanostructures for rapid hemostasis. However, when combined, additive manufacturing and electrospinning techniques<sup>[7]</sup> allow for the possibility and the ease of selecting different types of materials to enable the fabrication of specifically designed complex multiscale structures with multiple mesh layers and fiber densities (Figure 6A).

The material–cell biointerface is a significant aspect in combined micro/nanosurface modification methods for hemostat fabrication. This is because the mechanical interactions between a cell and its surrounding biochemical and biophysical environment influence cell behavior and function. When combining 3D printing with electrospinning, modifications are possible due to the choice of material in fabrication, solution viscosity, and internal mechanochemical interactions. Different 3D-printed substrates, such as steel, plastic, and glass, demonstrate varying levels of shear strength concerning displacement when a force is applied, impacting cellular kinetics. We can see mechanical-induced deformation due to the stretching and relaxation of an alginate hydrogel on the 3D-printed scaffold shown in Figure 6B. Such electrospun fiber mats can also be inlaid with cells or particles before incorporation into the 3D-printed scaffold to tune the desired effect of the resultant hemostat. This further enhances a fabricated agent's hemostatic capacities by preventing blood loss and reducing hemostasis time<sup>[88,107]</sup>. As shown in Figure 6C, an electrospun nanofiber mat is combined with a 3D-printed scaffold to create a 3D nanofibrous scaffold for rapid hemostasis<sup>[94]</sup>.

Other examples showing the beneficial results of combined fabrication include developing electrospun multiwall carbon nanotubes grafted to a 3D-printed oxidized regenerated cellulose gauze. Hemostatic evaluation of a similar electrospun sponge can be seen in Figure 6D. Meanwhile, Figure 6E demonstrates how the morphology of a gelatin nanofiber sponge can be quickly restored after undergoing different degrees of compression<sup>[7]</sup>. The density and diameter of electrospun fibers on this 3D-printed

scaffold determine overall porosity. Porosity is directly proportional to water absorption levels. Therefore, this nanofiber sponge has a higher water absorption percentage than a less porous hemostatic membranous agent.

These recent examples show that the field of tissue engineering has significantly benefited from the combined use of 3D printing with electrospinning techniques. These combined technologies have allowed the fabrication of highly tunable hemostatic agents such as scaffolds inlaid with composite micro/nanostructures. Depending on the choice of fabrication techniques and materials, these agents can be fabricated with nanoscopic precision in their architecture, thus affecting their biophysical and mechanical properties<sup>[12,66]</sup>. Customized modules can also be fabricated in a patient-specific manner, thus helping to accelerate the natural wound healing and regenerative process on a case-by-case basis.

Every fabrication technique has advantages and limitations, so we must consider these aspects and appropriately select materials when designing micro/nanostructures for rapid hemostasis. Aside from 3D/4D printing, we can combine other additive manufacturing techniques with electrospinning to create micro/nanostructures with highly tunable characteristics. These techniques include extrusion methods<sup>[108,109]</sup>, stereolithography (SLA)<sup>[110]</sup>, and digital light processing (DLP)<sup>[56,111]</sup>. These fabrication methods are not as prevalent as inkjet 3D printing because most of them require the addition of processing additives, such as photoactive resins, which are not biocompatible and may damage the body. Furthermore, some fabrication techniques are incompatible with standard and valuable hemostatic materials. However, regardless of these drawbacks, extrusion methods, SLA, and DLP offer the advantage of high-resolution printing of features on the nanoscale level, along with other fabrication-specific benefits.

Extrusion-based printing methods use pneumatic air pressure or mechanical forces, which are generated using pistons or screws, respectively, to carve out user-defined 3D patterns from bio-inks. These printing methods fabricate chitosan-based bio-inks for 3D scaffold construction<sup>[105]</sup>. Gallium-based inks also influence blood clotting, enhance thrombin generation, and induce antibacterial activity<sup>[112]</sup>. Extrusion methods have been used for developing novel gallium-containing chitosan-based composite scaffolds as hemostatic agents<sup>[113]</sup>.

SLA is a laser-based printing technique that uses laser pulses to produce high-resolution, high-viscosity droplets on the printing surface<sup>[114]</sup>. Though the operating speed of SLA is slower compared to other printing methods, cells printed via this method experience less mechanical stress



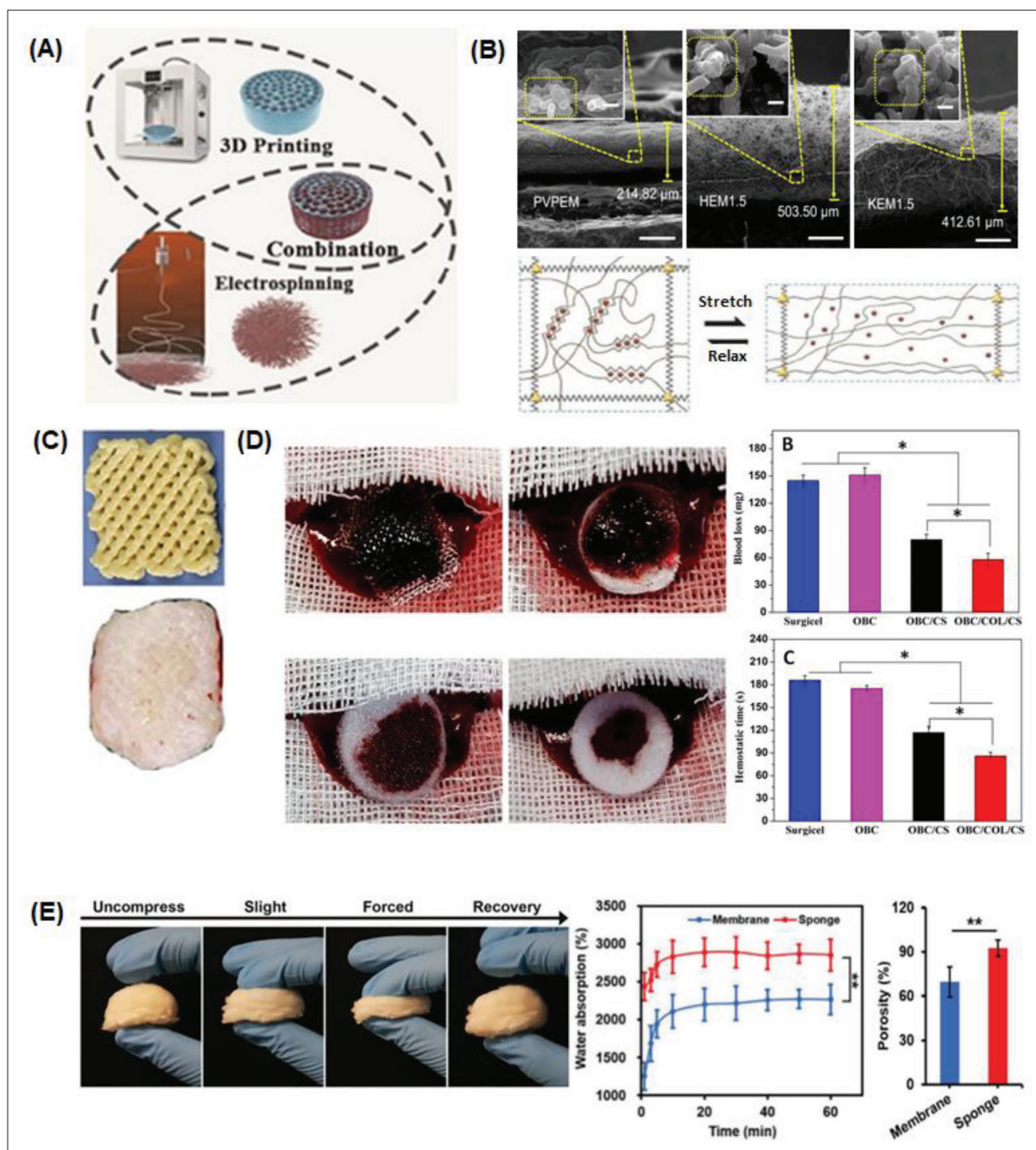


**Figure 6.** Combined methods of micro/nanosurface modification manufacture for rapid hemostasis. (A) 3D/4D printing and electrospinning techniques can be combined to achieve beneficial micro/nanosurface manipulations in hemostat fabrication<sup>[154]</sup>. (B) SEM images of electrospun nanoclay membranes: polyvinylpyrrolidone electrospun membrane (PVPEM), halloysite electrospun membrane (HEM), and kaolinite electrospun membrane (KEM)<sup>[14,41]</sup>. (C) Advanced fabrication for electrospun 3D nanofiber aerogels and scaffolds<sup>[94]</sup>. (D) Macroscopic images and subsequent evaluation of the hemostatic capacity of different electrospun sponges<sup>[107]</sup>. (E) A nanofiber sponge undergoing different degrees of compression. Water absorption and porosity percentages between the sponge and a membrane are compared<sup>[7]</sup>.

in fabrication, and thus, they have superior viability<sup>[105]</sup>. Therefore, SLA is used to print high-fidelity hydrogels<sup>[115]</sup> and highly complex nanocrystal composite hemostats given the high tunability of the structure made by SLA<sup>[116]</sup>.

DLP-based printing technologies utilize a projector to project the image of an object onto a free radical photosensitive liquid resin for high printing precision<sup>[117]</sup>. DLP is commonly used to fabricate hemostatic agents for

printing functional living skin. This method effectively incorporates living cells into hydrogel-based bio-inks to create topical wound dressings with excellent hemostatic potential and mechanical strength. This fabrication approach supports cell proliferation, migration, and subsequent skin regeneration by forming a suitable microenvironment mediated by air, moisture, and nutrient exchange<sup>[118]</sup>. Additionally, when combined with DLP printing, electrospun nanofiber-based scaffolds can provide cells with 3D microenvironments and biomimetic fibrous structures that promote tissue regeneration, thus enhancing the structural and bioactive effects of the resultant 3D-printed scaffold<sup>[14]</sup>.

Soft lithography is another fabrication technique utilized with other fabrication methods and additive manufacturing<sup>[119,120]</sup>. Soft lithography techniques can be utilized to create highly biomimetic, precise, and complex micro/nanostructures using popular hemostatic materials<sup>[47]</sup>. Thus, soft lithography methods are primarily employed in fabricating organ-on-a-chip platforms for drug development and personalized medicine applications<sup>[44]</sup> rather than hemostats adapted for clinical use<sup>[121]</sup>.

## 5. Hydrogels and cryogels as hemostats

Cryogels microspheres are one of the promising smart hemostatic materials that can deal with noncompressible bleeding within seconds. Such cryogels are reported to absorb blood within seconds. Zhan et al. reported the fabrication of cellulose@polydopamine/Thymol (Tm/Cell@PDA) cryogel microspheres ( $400 \pm 15 \mu\text{m}$ ) with shark skin riblet-inspired wrinkled surface to prevent acute bleeding within 10 seconds of application<sup>[122]</sup>. The fabricated cellulose microsphere could absorb blood six times its weight. Moreover, the microspheres could seal blood loss without applying pressure. A controlled freeze-drying technique customized the surface topology of the microspheres. Polydopamine (PDA) was incorporated into the microspheres by *in situ* polymerization rendering the microspheres tissue binding ability. Thymol in or on the microspheres contributed to the antibacterial activity. Upon application of the microspheres on acute bleeding, plasma is instantly drained, and blood components like RBCs, platelets, and coagulation factors are concentrated to accelerate the blood coagulation pathway. Wang et al. developed a hyaluronic acid-polyurethane (HA-PU) hybrid cryogel that is highly efficient in rapid hemostasis and wound healing. The PU emulsion and oxidized HA were autonomously cross-linked to form the hybrid cryogel at  $-20^\circ\text{C}$  through hydrazine bonding. The surface of the cryogel comprises macroporous structures of  $\sim 220 \mu\text{m}$  and, upon drying, could shrink up to 1/7 of its original volume. Due to its shape-memory property, the shrunk cryogel

could rapidly swell by 16 times upon blood absorption. The application of the cryogel was closely associated with the activation of the endogenous coagulation system, leading to hemostasis within 2 minutes of application<sup>[123]</sup>. Huang et al. reported the fabrication of numerous high-strength composite cryogel hemostats comprising PVA, carboxymethyl chitosan (CMCS), and dopamine (DA) (PVA/CMCS-DA). The variation in the concentration of the DA resulted in dramatic changes in the hemostatic ability of the prepared cryogel. The cryogel incorporated with 6 mg of DA exhibited favorable hemostatic ability by promoting the adhesion and activation of blood cells<sup>[124]</sup>. Teng et al. used the ice templating method to fabricate shape-recoverable gelatin/laponite nanoclay-based macroporous hydrogel hemostat. The fabricated macroporous hydrogel showed precise clotting ability as a noncompressible hemostat on liver bleeding. The rapid hemostasis is attained by the ability of the hydrogel to absorb blood, subsequently concentrating the coagulation factors. The incorporation of laponite nanoclay enables the activation of the endogenic coagulation cascade and accelerates thrombus formation. The prepared macroporous hydrogel displayed high affinity for blood cell in an irregular fashion. The irregular aggregation of the blood cells was linked to the interconnected porous structure with a high volume expansion ratio. The affinity of the hydrogel for the blood cells has primarily resulted from the anisotropic charge distribution of the nanoclay. The anisotropic charge distribution greatly enhances concentrating clotting factor, ultimately shortening blood coagulation time<sup>[125]</sup>. An antibacterial cryogel of sericin-methacryloyl/silver ions (SMC@Ag) was fabricated by Zhu et al. based on freeze polymerization of methacryloyl-modified sericin and the *in situ* reductions of silver ions. The Ag-incorporated interconnected micropores of the cryogel allows for high blood absorption and antibacterial activity in the cryogel. The hemostatic efficiency of the fabricated cryogel was better than commercial gelatin sponge in various *in vivo* set up, including rat tail amputation, liver injury, and femoral artery injury models. The hemostatic activity of the SMC@Ag cryogel was attributed to its ability to activate the coagulation pathway and enhancing the platelet adhesion during the coagulation process<sup>[126]</sup>. Injectable, antibacterial cryogel of chitosan (CS), oxidized gallic acid, and hemin (HE) was fabricated by Zhang et al. with high swelling efficiency upon application to the bleeding wound. Hemostatic efficiency of the cryogel was attributed to its high absorbency, blood cell and platelet adhesion ability, and shape recovery. The antibacterial property of the cryogel was observed upon exposure to NIR irradiation. The application of the cryogel significantly reduced inflammation, improved angiogenesis, and reduced wound healing time<sup>[127]</sup>. Bai et al. developed a multifunctional



single-component polymeric hydrogel of dopamine-modified poly(L-glutamate) with graphene oxide for rapid hemostasis and scarless wound healing. The hydrogel formation relied on oxidative catechol-crosslinking and catechol-carboxyl hydrogen bonding interactions. The resulting negative charge in the hydrogel rendered multifunctionality, including resistance to temperature, urea, and salt. Additionally, the hydrogel showed self-healing ability, injectability, desired adhesiveness, and detachability. The polymeric hydrogel could stop bleeding with 1.4% blood loss within 12 seconds<sup>[128]</sup>. An analysis of advantages and disadvantages of some other reported hemostats is given in Table 4.

## 6. Antimicrobial hemostats

An ideal hemostat with excellent antimicrobial properties is highly desirable for wound healing applications. Hemostatic materials can be functionalized with various antimicrobial drugs, metal nanoparticles, cationic antimicrobial polymers, or antimicrobial peptides for long-term antimicrobial effect<sup>[129,130]</sup>. Most antimicrobial agents kill the bacteria through cell wall disruption, membrane perforation, reactive oxygen species (ROS) generation, or ion leakage<sup>[129]</sup>. Photothermal antimicrobial agents exhibited hyperthermia-induced ROS generation and killing of bacterial pathogen<sup>[131]</sup>. For example, silver nanoparticle-doped alginate/chitosan hydrogel has been shown to promote diabetic wound healing, rapid hemostasis, and strong anti-bactericidal efficacy against *Escherichia coli* and *Pseudomonas aeruginosa*<sup>[132]</sup>.

Similarly, cyclohexane-modified N-halamine-doped chitosan sponge exhibited superior antibacterial effect within 10 minutes against *Staphylococcus aureus* and *E. coli*. Moreover, the fabricated sponge showed an extremely low blood clotting index with higher platelet adhesion activity<sup>[133,134]</sup>. Zhou et al. reported that a self-assembled antimicrobial peptide (jelleine-1) incorporated soft hydrogel to promote rapid hemostasis in a mouse liver injury model with fast blood clotting properties. The injectable hydrogel also displayed controlled platelet activation, adhesion, and blood coagulation owing to the presence of the J-1 peptide. Moreover, the fabricated hydrogel also showed substantial antibacterial properties against a broad range of bacteria (methicillin-resistant *S. aureus* [MRSA] and *E. coli*) and fungi (*Candida albicans*)<sup>[135]</sup>. Therefore, antimicrobial hemostats can be used as a potential alternative to commercial hemostats and provide a favorable environment for platelet adhesion and new tissue formation with robust antimicrobial properties<sup>[136]</sup>. Chen et al. reported the fabrication of adhesive, self-healing, and antibacterial hydrogel of gelatin methacrylate, adenine acrylate, and  $\text{CuCl}_2$  for diabetic wound healing.

The self-healing and adhesive properties were attributed to the hydrogen bond and metal-ligand coordination provided by the copper ion and carboxyl groups. An increased concentration of  $\text{Cu}^{2+}$  in the fabricated hydrogel was reported to inhibit the growth of *S. aureus* and *E. coli* within 3 hours of incubation. The antibacterial efficiency of the hydrogel was contributed by the ability of the  $\text{Cu}^{2+}$  to destroy bacterial cell membranes and alter protein and enzyme structures<sup>[137]</sup>. Yu et al. developed supramolecular thermo-contracting adhesive hydrogel effective against MRSA infection during wound healing. The antimicrobial hemostat was fabricated via host-guest interaction using quaternized chitosan-graft- $\beta$ -cyclodextrin, adenine, and polypyrrole nanotubes. The multifunctionality of the developed hemostat could achieve significant hemostasis and subsequent wound healing within 24 hours post-surgery<sup>[138]</sup>. Liang et al. reported the development of multifunctional hydrogel dressing comprising numerous functional materials, rendering it great adhesive property, antibacterial efficiency, antioxidative ability, conductivity, pH/glucose dual-responsive drug release properties, and effective against athletic diabetic foot wounds<sup>[139]</sup>. All the hydrogels mentioned above hold numerous possibilities for clinical application and improvement in the healthcare unit.

## 7. Conclusion

This review expounds various ways of utilizing micro/nanostructures for hemostatic applications in different cases, including civilian settings and instances of heavy and complex surgeries<sup>[66]</sup>. Recent advances in 3D printing technologies have facilitated the fabrication of more precise scaffolds for this purpose via various micro/nanostructures, including nanotubes, nanofibers, micro/nanoparticles, micro/nanospheres, and adhesive powders/gels. We reviewed how different modeling methods, printing materials, and preparation techniques benefit in unison with 3D and 4D printing technologies. Although electrospinning is the most common pairing for 3D/4D printing, it is also possible to combine these printing techniques with others such as extrusion methods, soft lithography, SLA, and DLP-based methods in the construction of novel micro/nanostructures for rapid hemostasis. Such techniques and applications have enabled advances in developing and prototyping hydrogel-based microfluidic chips<sup>[121]</sup>, composite hydrogel bioinks, organs-on-chips, and novel materials for hemostatic applications<sup>[19,44]</sup>.

We have seen the value of a successful active material and micro/nanostructure choice for hemostat fabrication. The purpose of such a successful material is threefold: (i) to support and enhance the tissue regeneration process at the

Table 4. Comparison between various hemostatic biomaterials with potential application and commercial hemostats

Reference hemostat (commercial)	Hemostat type/com-position	In vivo injury model	Time to hemostasis	Advantages	Reported disadvantages	Mechanism of action	References
Fibrin glue	Injectable/Hyaluronan conjugate with inorganic polyphosphate (HA-PolyP)	Mouse liver bleeding model	<5 minutes	Hemostatic efficiency similar to fibrin glue	None	Initiation of contact pathway of blood coagulation cascade, increased coagulation factor V activation, fibrin clot stabilization, promotion of factor XI feedback activation by thrombin	[229]
Fibrin glue	Injectable/Glycosylated catechol- and glucose-grafted poly(L-lysine) hydrogel	Liver hemorrhage model of SD male rat	<20 seconds	Strong tissue adhesion, good injectability, irregular shape filling ability, high performance hemostasis (outperforming fibrin glue), wound healing	Non-glycosylation leads to compromised biocompatibility	Hydrogel induced sealing of wound site by wet adhesion, higher absorption of RBCs and platelets	[186]
Fibrin sealant and floseal	Injectable/Potassium aluminum sulfate (PA) and calcium chloride (Ca) entrapped chitosan based composite hydrogel (Cs-PA-Ca)	Rat liver and femoral artery hemorrhage model	Cs-PA-Ca (20 ± 10 seconds, 105 ± 31 seconds), Fibrin sealant (77 ± 26 seconds, 204 ± 58 seconds), Floseal (76 ± 15 seconds, 218 ± 46 seconds)	Faster blood clot formation over commercial hemostats	Material retention even after 8-weeks post-surgery	Accelerated platelet/RBC aggregation, activation of the coagulation cascade	[230]
Gelatin sponge	Subcutaneous implantation/ chitin-glucan composite sponge	Rat femoral artery, non-compressive liver puncture injury model	<60 seconds	Higher hemostatic efficiency over commercial hemostat, robust mechanical property, blood triggered shape memory	None	RBC aggregation, accelerated collagen synthesis, and new blood vessel formation	[231]
Surgicel, Curaspon	Chitosan loaded β-cyclodextrin polyester (CDPE-Cs) hydrogel	Liver punch biopsy model in rats, rabbits, pigs	-	Higher hemostatic efficiency than commercial hemostats	-	-	[232]
ChitoGauze <sup>®</sup> XR and Spongostan <sup>™</sup>	Graphene oxide (GO)/chitosan (CS)/ gelatin (GEL)/ polyvinyl alcohol (PVA) based aerogel	Rat tail amputation model	Coagulation up to 95% within 240 seconds	Faster hemostasis over commercial hemostat by ~4-5 times	None	Activation of erythrocytes and platelets on the aerogel surface	[233]
Celox <sup>®</sup>	Iota-carrageenan/xyloglucan/serine powder incorporate with tranexamic acid (IC:XYL:SER:TA-x%)	Rat tail amputation model	IC:XYL:SER:TA-2%: 136.2 ± 14.0 seconds Celox <sup>®</sup> : 129.4 ± 18.9 seconds	Hemostatic efficiency comparable to Celox <sup>®</sup> , Light weight, easy to use, antibacterial, anti-oxidative, promising alternative for controlling external bleeding	Hemostasis performance in large mammals might be advantageous	Enhanced adhesion of RBC	[234]

wound or defect site; (ii) to degrade *in situ* with minimal adverse effects; and (iii) to eventually get replaced with the body's own newly generated tissue. Therefore, to increase the biofunctional potential of these novel agents, there is a need to fabricate scaffolds that can recreate the micro/nanoscale topographical landscape while considering the role of bioactive factors that react to cues from the extracellular environment<sup>[6,14,140]</sup>. For this purpose, we have specifically designed and seamlessly integrated micro/nanostructures into multilayered scaffolds because of their inherent ability to closely reflect the body's natural physiologic processes in injured tissues<sup>[37]</sup>.

To further elucidate these bioactive interactions between material properties and behavior, computational models and high-throughput experimentation can serve as a potential tool to accelerate the development of high-performance materials and confirm micro/nanostructure interactions in the cell–matrix interface<sup>[141,142]</sup>. Other applications include using a nonlinear finite element code analysis to conduct simulations to study the mechanics of submicron pillars and cell interaction when considering different substrates as potential high-performance materials<sup>[6,143]</sup>.

One of these high-performance materials for hemostasis and wound healing is hydrogels. Hydrogels have the inherent advantages of injectability, self-healing, and remodeling. We can combine them with printed micro/nanostructures for rapid hemostasis promotion and an overall biomimetic wound healing effect. When designed together with stimulus-responsive capabilities, such as pH and ROS sensitivity<sup>[41]</sup>, these novel hydrogel constructs gain the ability to realize sequential and on-demand drug delivery<sup>[74,144]</sup>. Additionally, the surface topographical features and chemical composition of micro/nanostructures, such as biodegradable CNFs, can be further documented to develop advanced design strategies for more effective hemostatic products with on-demand drug delivery capabilities for future clinical use<sup>[37]</sup>.

This sequential and on-demand drug delivery has been made possible by recent advancements in tissue engineering and regenerative medicine and elucidating the beneficial effects of micro/nanostructures. Recently, we have seen much growth in the development of multifunctional intelligent materials for advanced therapeutic applications<sup>[145]</sup>. Currently available technologies allow us to accurately and precisely mimic distinct characteristics in the *in situ* microenvironment using different materials and development methods for user-tunable micro/nanostructures. *In vivo* tissue architecture is very complex and dynamic, as there is much interconnectivity between cells and specific components of the extracellular matrix<sup>[18]</sup>.

Therefore, to achieve the best biodegradable and bioactive effects compatible with typical human physiology, it is imperative to elucidate the structure and composition of the ECM to develop more efficient and effective micro/nanostructures<sup>[146]</sup>.

## 8. Future prospects

There are many advantages to utilizing micro/nanostructures for hemostasis and wound healing applications. We can combine novel technologies such as 3D/4D printing and electrospinning to fabricate biomimetic hemostatic agents that assist the body's natural regenerative responses when it cannot do so on its own. Because of this, 3D/4D printing techniques are a significant step in advancing from generalized administration of medications and therapy to personalized therapy for hemostasis and wound healing applications<sup>[7,147]</sup>.

We can potentially bring the benefits of efficient and effective cellular and molecular healing techniques via micro/nanostructures to civilian and surgical settings where wounds, surgery, and even hemophilia are relatively common. We will continue to develop more effective and targeted hemostatic agents for more biomimetic, patient-specific therapies using the combined technologies, active biomolecules and mediators, stimulus responsivity, and biophysical signaling applications available to supplement the design of micro/nanostructures.

However, there remains a shortage of information on the mechanisms of action and progression of *in situ* cell behavior, mainly owing to the shortage of detection tools to precisely monitor cell behavior in internal conditions. Thus, research teams are striving to enable the detection of bio-relevant analytes for such signaling purposes by incorporating micro/nanostructures into sensing systems. For example, a 2020 study by García-Astrain et al.<sup>[148]</sup> described the potential of using a surface-enhanced Raman scattering (SERS) spectroscopy within a plasmonic hydrogel-based, 3D-printed scaffold to this end. These SERS-active scaffolds allow for the 3D detection of model molecules and biomarkers and offer great flexibility in selecting plasmonic nanoparticles. Additionally, this study proved the possibility of using these plasmonic scaffolds for SERS sensing of cell-secreted molecules over extended periods by detecting the biomarker adenosine for biosensing applications<sup>[148]</sup>. Other studies have highlighted different methods of triggering local sensing based on micro/nanostructures' stimulus-responsive capacities using external signals, such as light via laser<sup>[147]</sup>, temperature<sup>[89]</sup>, ultrasound, or an applied magnetic field.

Such a biosensing method is crucial to advancing wound healing technologies because foreign-body

responses caused by implanted materials are significant obstacles to fabricated agents and devices<sup>[149,150]</sup>. We must also consider the dynamic environment of the ECM and the ways changes in fabricated micro/nanostructures can potentially affect the physical, biochemical, and bioactive properties of biodegradable materials in *in situ* scenarios<sup>[151]</sup>. Nevertheless, the body's natural immunomodulating responses still present significant obstacles in developing implantable materials and medical devices, especially for safe and effective clinical use<sup>[82]</sup>. Fortunately, advances in the hemostatic mechanisms of micro/nanostructures have provided strategies to resist the foreign-body response. Novel elucidations will serve to develop novel strategies to further mitigate such negative responses in the future<sup>[149]</sup>.

## Acknowledgments

Not applicable.

## Funding

This work was supported by the 'Basic Science Research Program' through the 'National Research Foundation of Korea' funded by the Ministry of Education (NRF-2018R1A16A1A03025582, NRF-2019R1D1A3A03103828, and NRF-2022R1I1A3063302).

## Conflict of interest

The authors declare no conflicts of interest.

## Author contributions

*Conceptualization:* Keya Ganguly, Maria Mercedes Espinal

*Investigation:* Keya Ganguly, Maria Mercedes Espinal

*Writing – original draft:* Keya Ganguly, Maria Mercedes Espinal

*Writing – review & editing:* Keya Ganguly, Sayan Deb Dutta, Dinesh K. Patel, Tejal V. Patil, Rachmi Luthfikasari

*Funding acquisition:* Ki-Taek Lim

*Project administration:* Ki-Taek Lim

*Supervision:* Ki-Taek Lim

## Ethics approval and consent to participate

Not applicable.

## Consent for publication

Not applicable.

## Availability of data

Not applicable.

## References

1. Phillips R, Friberg M, Lantz Cronqvist M, *et al.*, 2020, Visual blood loss estimation accuracy: Directions for future research based on a systematic literature review. *Proceedings of the human factors and ergonomics society annual meeting*: Sage Publications, Los Angeles, CA, 1411–1415.
2. Granville-Chapman J, Jacobs N, Midwinter M, 2011, Pre-hospital haemostatic dressings: A systematic review. *Injury*, 42: 447–459.
3. Du X, Wu L, Yan H, *et al.*, Microchannelled alkylated chitosan sponge to treat noncompressible hemorrhages and facilitate wound healing. *Nat Commun*, 12: 4733.
4. Zheng DW, Hong S, Xu L, *et al.*, 2018, Hierarchical micro-/nanostructures from human hair for biomedical applications. *Adv Mater*, 30: e1800836.
5. He J, Liang Y, Shi M, *et al.*, 2020, Anti-oxidant electroactive and antibacterial nanofibrous wound dressings based on poly( $\epsilon$ -caprolactone)/quaternized chitosan-graft-polyaniline for full-thickness skin wound healing. *J Chem Eng*, 385: 123464.
6. Nouri-Goushki M, Angeloni L, Modaresifar K, *et al.*, 2021, 3D-printed submicron patterns reveal the interrelation between cell adhesion, cell mechanics, and osteogenesis. *ACS Appl Mater Interfaces*, 13: 33767–33781.
7. Xie X, Li D, Chen Y, *et al.*, 2021, Conjugate electrospun 3D gelatin nanofiber sponge for rapid hemostasis. *Adv Healthc Mater*, 10, e2100918.
8. Wang K, Dong R, Tang J, *et al.*, 2021, Exosomes laden self-healing injectable hydrogel enhances diabetic wound healing via regulating macrophage polarization to accelerate angiogenesis. *J Chem Eng*, 430: 132664.
9. Wang Z, Agrawal P, Zhang YS, 2021, Nanotechnologies and nanomaterials in 3D (Bio)printing toward bone regeneration. *Adv NanoBio Res*, 1: 2100035.
10. Sun X, Bai Y, Zhai H, *et al.*, 2019, Devising micro/nano-architectures in multi-channel nerve conduits towards a pro-regenerative matrix for the repair of spinal cord injury. *Acta Biomater*, 86: 194–206.
11. Li M, Liang Y, Liang Y, *et al.*, 2022, Injectable stretchable self-healing dual dynamic network hydrogel as adhesive anti-oxidant dressing for photothermal clearance of bacteria and promoting wound healing of MRSA infected motion wounds. *J Chem Eng*, 427: 132039.
12. Xie C, Ye J, Liang R, *et al.*, 2021, Advanced strategies of biomimetic tissue-engineered grafts for bone regeneration. *Adv Healthc Mater*, 10: e2100408.
13. Nam S, Mooney D, 2021, Polymeric tissue adhesives. *Chem Rev*, 121:11336–11384.
14. Wan X, Liu Z, Li L, 2021, Manipulation of stem cells fates: The master and multifaceted roles of biophysical cues of biomaterials. *Adv Funct Mater*, 31: 2010626.



15. Mao AS, Özkalea B, Shah NJ, *et al.*, 2019, Programmable microencapsulation for enhanced mesenchymal stem cell persistence and immunomodulation. *PNAS*, 116: 15392–15397.
16. Jia X, Minami K, Uto K, *et al.*, 2020, Adaptive liquid interfacially assembled protein nanosheets for guiding mesenchymal stem cell fate. *Adv Mater*, 32: e1905942.
17. Ma Y, Jiang L, Hu J, *et al.*, 2020, Multifunctional 3D microstructures fabricated through temporally shaped femtosecond laser processing for preventing thrombosis and bacterial infection. *ACS Appl Mater Interfaces*, 12: 17155–17166.
18. Mariano A, Lubrano C, Bruno U, *et al.*, 2021, Advances in cell-conductive polymer biointerfaces and role of the plasma membrane. *Chem Rev*, 122: 4552–4580.
19. Guo B, Dong R, Liang Y, *et al.*, 2021, Haemostatic materials for wound healing applications. *Nat Rev Chem*, 5: 773–791.
20. Sakurai Y, Hardy ET, Ahn B, *et al.*, 2018, A microengineered vascularized bleeding model that integrates the principal components of hemostasis. *Nat Commun*, 9: 509.
21. Wilgus TA, Roy S, McDaniel JC, 2013, Neutrophils and wound repair: Positive actions and negative reactions. *Adv Wound Care*, 2: 379–388.
22. Davies LC, Jenkins SJ, Allen JE, *et al.*, 2013, Tissue-resident macrophages. *Nat Immun*, 14: 986–995.
23. Ansell DM, Izeta A, 2015, Pericytes in wound healing: Friend or foe? *Exp Dermatol*, 24: 833–834.
24. Armulik A, Genové G, Betsholtz C, 2011, Pericytes: Developmental, physiological, and pathological perspectives, problems, and promises. *Dev Cell*, 21: 193–215.
25. Crisan M, Yap S, Casteilla L, *et al.*, 2008, A perivascular origin for mesenchymal stem cells in multiple human organs. *Cell Stem Cell*, 3: 301–313.
26. Asahara T, Murohara T, Sullivan A, *et al.*, 1997, Isolation of putative progenitor endothelial cells for angiogenesis. *Science*, 275: 964–966.
27. Ceradini DJ, Kulkarni AR, Callaghan MJ, *et al.*, 2004, Progenitor cell trafficking is regulated by hypoxic gradients through HIF-1 induction of SDF-1. *Nat Med*, 10: 858–864.
28. Kosaraju R, Rennert RC, Maan ZN, *et al.*, 2016, Adipose-derived stem cell-seeded hydrogels increase endogenous progenitor cell recruitment and neovascularization in wounds. *Tissue Eng Part A*, 22: 295–305.
29. Tepper OM, Capla JM, Galiano RD, *et al.*, 2005, Adult vasculogenesis occurs through in situ recruitment, proliferation, and tubulization of circulating bone marrow-derived cells. *Blood*, 105: 1068–1077.
30. Donati G, Rognoni E, Hiratsuka T, *et al.*, 2017, Wounding induces dedifferentiation of epidermal Gata6+ cells and acquisition of stem cell properties. *Nat Cell Biol*, 19: 603–613.
31. Hsu C, Hutt E, Bloomfield DM, *et al.*, 2021, Factor XI inhibition to uncouple thrombosis from hemostasis: JACC review topic of the week. *J Am Coll Cardiol*, 78: 625–631.
32. Liu J, Solanki A, White MJ, *et al.*, 2022, Therapeutic use of  $\alpha$ 2-antiplasmin as an antifibrinolytic and hemostatic agent in surgery and regenerative medicine. *NPJ Regen Med*, 7: 1–11.
33. Neubauer K, Zieger B, 2021, Endothelial cells and coagulation. *Cell Tissue Res*, 7: 1–8.
34. Law LA, Graham DK, Di Paola J, 2018, GAS6/TAM pathway signaling in hemostasis and thrombosis. *Front Med*, 5: 137.
35. Weisel J, Litvinov R, 2019, Red blood cells: The forgotten player in hemostasis and thrombosis. *J Thromb Haemost*, 17: 271–282.
36. Rodrigues M, Kosaric N, Bonham CA, *et al.*, 2019, Wound healing: A cellular perspective. *Physiol Rev*, 99: 665–706.
37. Abdi MM, Razalli RL, Tahir PM, *et al.*, 2019, Optimized fabrication of newly cholesterol biosensor based on nanocellulose. *Int J Biol Macromol*, 126: 1213–1222.
38. Freedman BR, Uzun O, Luna NMM, *et al.*, 2021, Degradable and removable tough adhesive hydrogels. *Adv Mater*, 33: e2008553.
39. Feng Y, Luo X, Wu F, *et al.*, 2022, Systematic studies on blood coagulation mechanisms of halloysite nanotubes-coated PET dressing as superior topical hemostatic agent. *J Chem Eng*, 428: 132049.
40. Long M, Zhang Y, Huang P, *et al.*, 2018, Emerging nanoclay composite for effective hemostasis. *Adv Funct Mater*, 28: 1704452.
41. Cui Y, Huang Z, Lei L, *et al.*, 2021, Robust hemostatic bandages based on nanoclay electrospun membranes. *Nat Commun*, 12: 5922.
42. Zhang Y, Li C, Zhang W, *et al.*, 2021, 3D-printed NIR-responsive shape memory polyurethane/magnesium scaffolds with tight-contact for robust bone regeneration. *Bioact Mater*, 16–218–231.
43. Liang Y, He J, Guo B, 2021, Functional hydrogels as wound dressing to enhance wound healing. *ACS Nano*, 15: 12687–12722.
44. Bhusal A, Dogan E, Nguyen HA, *et al.*, 2021, Multi-material digital light processing bioprinting of hydrogel-based microfluidic chips. *Biofabrication*, 14: 1–14.
45. Lei C, Xie Z, Wu K, *et al.*, 2021, Controlled vertically aligned structures in polymer composites: Natural inspiration, structural processing, and functional application. *Adv Mater*, 33: e2103495.
46. Chaudhuri O, Cooper-White J, Janmey PA, *et al.*, 2020, Effects of extracellular matrix viscoelasticity on cellular behaviour. *Nature*, 584: 535–546.
47. McHugh KJ, Nguyen TD, Linehan AR, *et al.*, 2017, Fabrication of fillable microparticles and other complex 3D microstructures. *Science*, 357: 1138–1142.

48. Chen S, Carlson MA, Zhang YS, *et al.*, 2018, Fabrication of injectable and superelastic nanofiber rectangle matrices (“peanuts”) and their potential applications in hemostasis. *Biomaterials*, 179: 46–59.
49. Chen R, Zhao C, Chen Z, *et al.*, 2022, A bionic cellulose nanofiber-based nanocage wound dressing for NIR-triggered multiple synergistic therapy of tumors and infected wounds. *Biomaterials*, 281: 121330.
50. Jeong GJ, Im GB, Lee TJ, *et al.*, 2021, Development of a stem cell spheroid-laden patch with high retention at skin wound site. *Bioeng Transl Med*, 2022: 1–10.
51. Shi Z, Lan G, Hu E, *et al.*, 2022, Targeted delivery of hemostats to complex bleeding wounds with magnetic guidance for instant hemostasis. *J Chem Eng*, 427: 130916.
52. Xi G, Liu W, Chen M, *et al.*, 2019, Polysaccharide-based lotus seedpod surface-like porous microsphere with precise and controllable micromorphology for ultrarapid hemostasis. *ACS Appl Mater Interfaces*, 11: 46558–46571.
53. Huang X, Fu Q, Deng Y, *et al.*, 2021, Surface roughness of silk fibroin/alginate microspheres for rapid hemostasis in vitro and in vivo. *Carbohydr Polym*, 253: 117256.
54. Liu X, Moradi MA, Bus T, *et al.*, 2021, Flower-like colloidal particles through precipitation polymerization of redox-responsive liquid crystals. *Angew Chem*, 60: 27026–27030.
55. Lv C, Li L, Jiao Z, *et al.*, 2021, Improved hemostatic effects by Fe(3+) modified biomimetic PLLA cotton-like mat via sodium alginate grafted with dopamine. *Bioact Mater*, 6: 2346–2359.
56. Wu J, Guo J, Linghu C, *et al.*, 2021, Rapid digital light 3D printing enabled by a soft and deformable hydrogel separation interface. *Nat Commun*, 12: 6070.
57. Peng X, Xu X, Deng Y, *et al.*, 2021, Ultrafast self-gelling and wet adhesive powder for acute hemostasis and wound healing. *Adv Funct Mater*, 31: 2102583.
58. Collins MN, Ren G, Young K, *et al.*, 2021, Scaffold fabrication technologies and structure/function properties in bone tissue engineering. *Adv Funct Mater*, 31: 2010609.
59. Mohamed E, Fitzgerald A, Tsuzuki T, 2021, The role of nanoscale structures in the development of topical hemostatic agents. *Mater Today Nano*, 16: 100137.
60. Karavasilis C, Fatouros DG, 2021, Self-assembling peptides as vectors for local drug delivery and tissue engineering applications. *Adv Drug Deliv Rev*, 174: 387–405.
61. Udangawa RN, Mikael PE, Mancinelli C, *et al.*, 2019, Novel cellulose-halloysite hemostatic nanocomposite fibers with a dramatic reduction in human plasma coagulation time. *ACS Appl Mater Interfaces*, 11: 15447–15456.
62. Sun X, Jia P, Zhang H, *et al.*, 2021, Green regenerative hydrogel wound dressing functionalized by natural drug-food homologous small molecule self-assembled nanospheres. *Adv Funct Mater*, 32: 2106572.
63. Yuk H, Wu J, Sarrafian TL, *et al.*, 2021, Rapid and coagulation-independent haemostatic sealing by a paste inspired by barnacle glue. *Nat Biomed Eng*, 5: 1131–1142.
64. Yang Y, Liang Y, Chen J, *et al.*, 2022, Mussel-inspired adhesive antioxidant antibacterial hemostatic composite hydrogel wound dressing via photo-polymerization for infected skin wound healing. *Bioact Mater*, 8: 341–354.
65. Ruiz-Esparza GU, Wang X, Zhang X, *et al.*, 2021, Nanoengineered shear-thinning hydrogel barrier for preventing postoperative abdominal adhesions. *Micro Nano Lett*, 13: 212.
66. Pourshahrestani S, Zeimaran E, Kadri NA, *et al.*, 2020, Polymeric hydrogel systems as emerging biomaterial platforms to enable hemostasis and wound healing. *Adv Healthc Mater*, 9: e2000905.
67. Zhang F, King MW, 2020, Biodegradable polymers as the pivotal player in the design of tissue engineering scaffolds. *Adv Healthc Mater*, 9:e1901358.
68. Wang XX, Liu Q, Sui JX, *et al.*, 2019, Recent advances in hemostasis at the nanoscale. *Adv Healthc Mater*, 8: e1900823.
69. Hao R, Peng X, Zhang Y, *et al.*, 2020, Rapid hemostasis resulting from the synergism of self-assembling short peptide and O-carboxymethyl chitosan. *ACS Appl Mater Interfaces*, 12: 55574–55583.
70. Vassey MJ, Figueredo GP, Scurr DJ, *et al.*, 2020, Immune modulation by design: Using topography to control human monocyte attachment and macrophage differentiation. *Adv Sci*, 7: 1903392.
71. Zhou K, Chigan D, Xu L, *et al.*, 2021, Anti-sandwich structured photo-electronic wound dressing for highly efficient bacterial infection therapy. *Small*, 17: e2101858.
72. Chen M, Dong R, Zhang J, *et al.*, 2021, Nanoscale metal-organic frameworks that are both fluorescent and hollow for self-indicating drug delivery. *ACS Appl Mater Interfaces*, 13: 18554–18562.
73. Gong, Celi N, Zhang D, 2022, Magnetic biohybrid microrobot multimers based on chlorella cells for enhanced targeted drug delivery. *ACS Appl Mater Interfaces*, 14: 6320–6330.
74. Chen J, Caserto JS, Ang I, *et al.*, 2021, An adhesive and resilient hydrogel for the sealing and treatment of gastric perforation. *Bioact Mater*, 14: 52–60.
75. Wang J, Li Y, Nie G, 2021, Multifunctional biomolecule nanostructures for cancer therapy. *Nat Rev Mater*, 6: 1–18.
76. Daikuara LY, Chen X, Yue Z, *et al.*, 2021, 3D bioprinting constructs to facilitate skin regeneration. *Adv Funct Mater*, 32: 2105080.
77. Li D, Yang Z, Zhao X, *et al.*, 2022, Osteoimmunomodulatory injectable lithium-heparin hydrogel with microspheres/TGF- $\beta$ 1 delivery promotes M2 macrophage polarization and osteogenesis for guided bone regeneration. *J Chem Eng*, 435: 134991.

78. Nasajpour A, Mandla S, Shree S, *et al.*, 2017, Nanostructured fibrous membranes with rose spike-like architecture. *Nano Lett*, 17:6235–6240.
79. Liang Y, Li Z, Huang Y, *et al.*, 2021, Dual-dynamic-bond cross-linked antibacterial adhesive hydrogel sealants with on-demand removability for post-wound-closure and infected wound healing. *ACS Nano*, 15: 7078–7093.
80. Hu Y, Cao S, Chen J, *et al.*, 2020, Biomimetic fabrication of icariin loaded nano hydroxyapatite reinforced bioactive porous scaffolds for bone regeneration. *J Chem Eng*, 394: 124895.
81. Liverani L, Liguori A, Zezza P, *et al.*, 2021, Nanocomposite electrospun fibers of poly( $\epsilon$ -caprolactone)/bioactive glass with shape memory properties. *Bioact Mater*, 11: 230–239.
82. Adu-Berchie K, Mooney DJ, 2020, Biomaterials as local niches for immunomodulation. *Acc Chem Res*, 53: 1749–1760.
83. Li Y, Niu F, Zhao X, *et al.*, 2021, Nonwetting nanostructured hemostatic material for bleeding control with minimal adhesion. *Adv Mater Interfaces*, 8: 2101412.
84. Yan Y, Yan J, Gong X, *et al.*, 2021, All-in-one asymmetric micro-supercapacitor with negative Poisson's ratio structure based on versatile electrospun nanofibers. *J Chem Eng*, 133580.
85. Guo Y, Huang J, Fang Y, *et al.*, 2022, 1D, 2D, and 3D scaffolds promoting angiogenesis for enhanced wound healing. *J Chem Eng*, 437: 134690.
86. Yang G, Kong H, Chen Y, *et al.*, 2022, Recent advances in the hybridization of cellulose and carbon nanomaterials: Interactions, structural design, functional tailoring, and applications. *Carbohydr Polym*, 279: 118947.
87. Wang L, Zhou M, Xu T, *et al.*, 2022, Multifunctional hydrogel as wound dressing for intelligent wound monitoring. *J Chem Eng*, 433: 134625.
88. Yang H, Liang Y, Wang J, *et al.*, 2021, Multifunctional wound dressing for rapid hemostasis, bacterial infection monitoring and photodynamic antibacterial therapy. *Acta Biomater*, 135: 179–190.
89. Khodaei A, Jahanmard F, Madaah Hosseini HR, *et al.*, 2021, Controlled temperature-mediated curcumin release from magneto-thermal nanocarriers to kill bone tumors. *Bioact Mater*, 11: 107–117.
90. Zheng L, Wang Q, Zhang YS, *et al.*, 2021, A hemostatic sponge derived from skin secretion of *Andrias davidianus* and nanocellulose. *J Chem Eng*, 416: 129136.
91. Li Y, Zhu J, Cheng H, *et al.*, 2021, Developments of advanced electrospinning techniques: A critical review. *Adv Mater Technol*, 6: 2100410.
92. Zheng Y, Ma W, Yang Z, *et al.*, 2022, An ultralong hydroxyapatite nanowire aerogel for rapid hemostasis and wound healing. *J Chem Eng*, 430: 132912.
93. Zhang X, Lei Y, Li C, *et al.*, 2021, Superhydrophobic and multifunctional aerogel enabled by bioinspired salvinia leaf-like structure. *Adv Funct Mater*, 32: 2110830.
94. Chen Y, Shafiq M, Liu M, *et al.*, 2020, Advanced fabrication for electrospun three-dimensional nanofiber aerogels and scaffolds. *Bioact Mater*, 5: 963–979.
95. Tafreshi OA, Mosanenzadeh SG, Karamikamkar S, *et al.*, 2022, A review on multifunctional aerogel fibers: Processing, fabrication, functionalization, and applications. *Mater Today Chem*, 23: 100736.
96. Zhang X, Li Y, He D, *et al.*, 2021, An effective strategy for preparing macroporous and self-healing bioactive hydrogels for cell delivery and wound healing. *J Chem Eng*, 425: 130677.
97. Wan Y, Han J, Cheng F, *et al.*, 2020, Green preparation of hierarchically structured hemostatic epoxy-amine sponge. *J Chem Eng*, 397: 125445.
98. Zhang K, Bai X, Yuan Z, *et al.*, 2019, Layered nanofiber sponge with an improved capacity for promoting blood coagulation and wound healing. *Biomater*, 204: 70–79.
99. Jiang J, Oguzlu H, Jiang F, 2021, 3D printing of lightweight, super-strong yet flexible all-cellulose structure. *J Chem Eng*, 405: 126668.
100. Hu Y, Wu B, Xiong Y, *et al.*, 2021, Cryogenic 3D printed hydrogel scaffolds loading exosomes accelerate diabetic wound healing. *J Chem Eng*, 426: 130634.
101. Zhang H, Cong Y, Osi AR, *et al.*, 2020, Direct 3D printed biomimetic scaffolds based on hydrogel microparticles for cell spheroid growth. *Adv Funct Mater*, 30: 1910573.
102. Zou F, Wang Y, Zheng Y, *et al.*, 2022, A novel bioactive polyurethane with controlled degradation and L-Arg release used as strong adhesive tissue patch for hemostasis and promoting wound healing. *Bioact Mater*, 17: 471–487.
103. Biranje SS, Sun J, Cheng L, *et al.*, 2022, Development of cellulose nanofibril/casein-based 3D composite hemostasis scaffold for potential wound-healing application. *ACS Appl Mater Interfaces*, 14: 3792–3808.
104. Pourchet LJ, Thepot A, Albouy M, *et al.*, 2017, Human skin 3D bioprinting using scaffold-free approach. *Adv Healthc Mater*, 6: 1–8.
105. Taghizadeh M, Taghizadeh A, Yazdi MK, *et al.*, 2022, Chitosan-based inks for 3D printing and bioprinting. *Green Chem*, 24: 62–101.
106. Lavrador P, Esteves MR, Gaspar VM, *et al.*, 2020, Stimuli-responsive nanocomposite hydrogels for biomedical applications. *Adv Funct Mater*, 31: 2005941.
107. Yuan H, Chen L, Hong FF, 2020, A biodegradable antibacterial nanocomposite based on oxidized bacterial nanocellulose for rapid hemostasis and wound healing. *ACS Appl Mater Interfaces*, 12: 3382–3392.
108. Placone JK, Engler AJ, 2018, Recent advances in extrusion-based 3d printing for biomedical applications. *Adv Healthc Mater*, 7: e1701161.

109. Davoodi E, Montazerian H, Zhianmanesh M, *et al.*, 2021, Template-enabled biofabrication of thick three-dimensional tissues with patterned perfusable macro-channels. *Adv Healthc Mater*, 2021: e2102123.
110. Weems AC, Arno MC, Yu W, *et al.*, 2021, 4D polycarbonates via stereolithography as scaffolds for soft tissue repair. *Nat Commun*, 12: 3771.
111. Cosola A, Sangermano M, Terenziani D, *et al.*, 2021, dlp 3D-printing of shape memory polymers stabilized by thermoreversible hydrogen bonding interactions. *Appl Mater Today*, 23: 101060.
112. Kurtuldu F, Mutlu N, Boccaccini AR, *et al.*, 2022, Gallium containing bioactive materials: A review of anticancer, antibacterial, and osteogenic properties. *Bioact Mater*, 17: 125–146.
113. Pourshahrestani S, Zeimaran E, Kadri NA, *et al.*, 2017, Potency and cytotoxicity of a novel gallium-containing mesoporous bioactive glass/chitosan composite scaffold as hemostatic agents. *ACS Appl Mater Interfaces*, 9: 31381–31392.
114. Galliger Z, Vogt CD, Panoskaltis-Mortari A, 2019, 3D bioprinting for lungs and hollow organs. *Transl Res*, 211: 19–34.
115. Sun Z, Lu Y, Zhao Q, *et al.*, 2022, A new stereolithographic 3D printing strategy for hydrogels with a large mechanical tunability and self-weldability. *Addit Manuf*, 50: 102563.
116. Palaganas NB, Mangadlao JD, de Leon ACC, *et al.*, 2017, 3D printing of photocurable cellulose nanocrystal composite for fabrication of complex architectures via stereolithography. *ACS Appl Mater Interfaces*, 9: 34314–34324.
117. Quan H, Zhang T, Xu H, *et al.*, 2020, Photo-curing 3d printing technique and its challenges. *Bioact Mater*, 5: 110–115.
118. Zhou F, Hong Y, Liang R, *et al.*, 2020, Rapid printing of bio-inspired 3D tissue constructs for skin regeneration. *Biomaterials*, 258: 120287.
119. Vera D, García-Díaz M, Torras N, *et al.*, Engineering tissue barrier models on hydrogel microfluidic platforms. *ACS Appl Mater Interfaces*, 13: 13920–13933.
120. Rezaei FS, Sharifianjazi F, Esmaeilkhani A, *et al.*, Chitosan films and scaffolds for regenerative medicine applications: A review. *Carbohydr Polym*, 273: 118631.
121. Illath K, Kar S, Gupta P, *et al.*, 2021, Microfluidic nanomaterials: From synthesis to biomedical applications. *Biomaterials*, 2021: 121247.
122. Xu Z, Tian W, Wen C, *et al.*, 2022, Cellulose-based cryogel microspheres with nanoporous and controllable wrinkled morphologies for rapid hemostasis. *Nano Letters*, 22: 6350–6358.
123. Wang M, Hu J, Ou Y, *et al.*, 2022, Shape-recoverable hyaluronic acid–waterborne polyurethane hybrid cryogel accelerates hemostasis and wound healing. *ACS Appl Mater Interfaces*, 14: 17093–17108.
124. Huang Y, Zhao X, Wang C, *et al.*, 2022, High-strength anti-bacterial composite cryogel for lethal noncompressible hemorrhage hemostasis: Synergistic physical hemostasis and chemical hemostasis. *J Chem Eng*, 427: 131977.
125. Teng L, Xia K, Qian T, *et al.*, 2022, Shape-recoverable macroporous nanocomposite hydrogels created via ice templating polymerization for noncompressible wound hemorrhage. *ACS Biomater Sci Eng*, 8: 2076–2087.
126. Zhu Y, Liu H, Qin S, *et al.*, 2022, Antibacterial sericin cryogels promote hemostasis by facilitating the activation of coagulation pathway and platelets. *Adv Healthc Mater*, 2022: 2102717.
127. Zhang Y, Wang Y, Chen L, *et al.*, An injectable antibacterial chitosan-based cryogel with high absorbency and rapid shape recovery for noncompressible hemorrhage and wound healing. *Biomaterials*, 285: 121546.
128. Bai Q, Teng L, Zhang X, *et al.*, 2022, Multifunctional single-component polypeptide hydrogels: The gelation mechanism, superior biocompatibility, high performance hemostasis, and scarless wound healing. *Adv Healthc Mater*, 11: 2101809.
129. Duan S, Wu R, Xiong Y-H, *et al.*, 2022, Multifunctional antimicrobial materials: From rational design to biomedical applications. *Prog Mater Sci*, 125: 100887.
130. Liu J, Zhou X, Zhang Y, *et al.*, 2022, Rapid hemostasis and excellent antibacterial cerium-containing mesoporous bioactive glass/chitosan composite sponge for hemostatic material. *Mater Today Chem*, 23: 100735.
131. Cao C, Yang N, Zhao Y, *et al.*, 2021, Biodegradable hydrogel with thermo-response and hemostatic effect for photothermal enhanced anti-infective therapy. *Nano Today*, 39: 101165.
132. Choudhary M, Chhabra P, Tyagi A, *et al.*, Scar free healing of full thickness diabetic wounds: A unique combination of silver nanoparticles as antimicrobial agent, calcium alginate nanoparticles as hemostatic agent, fresh blood as nutrient/growth factor supplier and chitosan as base matrix. *Int J Biol Macromol*, 178: 41–52.
133. Zheng Y, Pan N, Liu Y, *et al.*, 2021, Novel porous chitosan/N-halamine structure with efficient antibacterial and hemostatic properties. *Carbohydr Polym*, 253: 117205.
134. Yin M, Wang Y, Zhang Y, *et al.*, 2020, Novel quaternarized N-halamine chitosan and polyvinyl alcohol nanofibrous membranes as hemostatic materials with excellent antibacterial properties. *Carbohydr Polym*, 232: 115823.
135. Zhou J, Zhang H, Fareed MS, *et al.*, 2022, An injectable peptide hydrogel constructed of natural antimicrobial peptide j-1 and adp shows anti-infection, hemostasis, and antiadhesion efficacy. *ACS Nano*, 16: 7636–7657.
136. Liang Y, Liang Y, Zhang H, *et al.*, 2022, Antibacterial biomaterials for skin wound dressing. *Asian J Pharm Sci*, 17: 353–384.



137. Chen J, He J, Yang Y, *et al.*, 2022, Antibacterial adhesive self-healing hydrogels to promote diabetic wound healing. *Acta Biomater*, 146: 119–130.
138. Yu R, Li M, Li Z, *et al.*, 2022, Supramolecular thermocontracting adhesive hydrogel with self-removability simultaneously enhancing noninvasive wound closure and mrsa-infected wound healing. *Adv Healthc Mater*, 2022: 2102749.
139. Liang Y, Li M, Yang Y, *et al.*, 2022, Ph/glucose dual responsive metformin release hydrogel dressings with adhesion and self-healing via dual-dynamic bonding for athletic diabetic foot wound healing. *ACS Nano*, 16: 3194–3207.
140. Wang Y, Wu Y, Long L, *et al.*, 2021, Inflammation-responsive drug-loaded hydrogels with sequential hemostasis, antibacterial, and anti-inflammatory behavior for chronically infected diabetic wound treatment. *ACS Appl Mater Interfaces*, 13: 33584–33599.
141. Yang L, Pijuan-Galito S, Rho HS, *et al.*, 2021, High-throughput methods in the discovery and study of biomaterials and materiobiology. *Chem Rev*, 121: 4561–4677.
142. Khalil AS, Jaenisch R, Mooney DJ, 2020, Engineered tissues and strategies to overcome challenges in drug development. *Adv Drug Deliv Rev*, 158: 116–139.
143. Sun L, Yu Y, Chen Z, *et al.*, 2020, Biohybrid robotics with living cell actuation. *Chem Soc Rev*, 49: 4043–4069.
144. Kim K, Ryu Ji H, Koh M-Y, *et al.*, Coagulopathy-independent, bioinspired hemostatic materials: A full research story from preclinical models to a human clinical trial. *Sci Adv*, 7: eabc9992.
145. Gonzalez-Pujana A, Vining KH, Zhang DKY, *et al.*, 2020, Multifunctional biomimetic hydrogel systems to boost the immunomodulatory potential of mesenchymal stromal cells. *Biomaterials*, 257: 120266.
146. Ceylan H, Dogan NO, Yasa IC, *et al.*, 2021, 3D printed personalized magnetic micromachines from patient blood-derived biomaterials. *Sci Adv*, 7: eabh0273.
147. Geng H, Pan Yc, Zhang R, *et al.*, 2021, Binding to amyloid- $\beta$  protein by photothermal blood-brain barrier-penetrating nanoparticles for inhibition and disaggregation of fibrillation. *Adv Funct Mater*, 31: 2102953.
148. García-Astrain C, Lenzi E, Jimenez de Aberasturi D, *et al.*, 2020, 3D-printed biocompatible scaffolds with built-in nanoplasmonic sensors. *Adv Funct Mater*, 30: 2005407.
149. Zhang D, Chen Q, Shi C, *et al.*, 2020, Dealing with the foreign-body response to implanted biomaterials: Strategies and applications of new materials. *Adv Funct Mater*, 31: 2007226.
150. Balabiyev A, Podolnikova NP, Kilbourne JA, *et al.*, 2021, Fibrin polymer on the surface of biomaterial implants drives the foreign body reaction. *Biomaterials*, 277: 121087.
151. Lin X, Li F, Bing Y, *et al.*, 2021, Biocompatible multifunctional e-skins with excellent self-healing ability enabled by clean and scalable fabrication. *Micro Nano Lett*, 13: 200.
152. Kim JS, Hwang H, Lee D, *et al.*, 2021, Electrospinnable, neutral coacervates for facile preparation of solid phenolic bioadhesives. *ACS Appl Mater Interfaces*, 13: 37989–37996.
153. Li J, Celiz AD, Yang J, *et al.*, 2017, Tough adhesives for diverse wet surfaces. *Science*, 357: 378–381.
154. Wang Z, Wang Y, Yan J, *et al.*, 2021, Pharmaceutical electrospinning and 3D printing scaffold design for bone regeneration. *Adv Drug Deliv Rev*, 174: 504–534.
155. Chen J, Dai S, Liu L, *et al.*, 2021, Photo-functionalized TiO<sub>2</sub> nanotubes decorated with multifunctional Ag nanoparticles for enhanced vascular biocompatibility. *Bioact Mater*, 6: 45–54.
156. Cheng F, Liu C, Li H, *et al.*, 2018, Carbon nanotube-modified oxidized regenerated cellulose gauzes for hemostatic applications. *Carbohydr Polym*, 183: 246–253.
157. Leonhardt EE, Kang N, Hamad MA, *et al.*, 2019, Absorbable hemostatic hydrogels comprising composites of sacrificial templates and honeycomb-like nanofibrous mats of chitosan. *Nat Commun*, 10: 2307.
158. Yan J, Wang Y, Li X, *et al.*, 2021, A bionic nano-band-aid constructed by the three-stage self-assembly of peptides for rapid liver hemostasis. *Nano Lett*, 21: 7166–7174.
159. Madruga LYC, Popat KC, Balaban RC, *et al.*, 2021, Enhanced blood coagulation and antibacterial activities of carboxymethyl-kappa-carrageenan-containing nanofibers. *Carbohydr Polym*, 273: 118541.
160. Tavakoli S, Kharaziha M, Nemati S, *et al.*, 2021, Nanocomposite hydrogel based on carrageenan-coated starch/cellulose nanofibers as a hemorrhage control material. *Carbohydr Polym*, 251: 117013.
161. Mohamed E, Coupland LA, Crispin PJ, *et al.*, 2021, Non-oxidized cellulose nanofibers as a topical hemostat: In vitro thromboelastometry studies of structure vs function. *Carbohydr Polym*, 265: 118043.
162. Liu R, Dai L, Si C, *et al.*, 2018, Antibacterial and hemostatic hydrogel via nanocomposite from cellulose nanofibers. *Carbohydr Polym*, 195: 63–70.
163. Cheng F, Liu C, Wei X, *et al.*, 2017, Preparation and characterization of 2,2,6,6-tetramethylpiperidine-1-oxyl (tempo)-oxidized cellulose nanocrystal/alginate biodegradable composite dressing for hemostasis applications. *ACS Sustain Chem Eng*, 5: 3819–3828.
164. Lou P, Liu S, Wang Y, *et al.*, 2021, Injectable self-assembling peptide nanofiber hydrogel as a bioactive 3D platform to promote chronic wound tissue regeneration. *Acta Biomater*, 135: 100–112.

165. Adeli-Sardou M, Yaghoobi MM, Torkzadeh-Mahani M, *et al.*, 2019, Controlled release of lawsone from polycaprolactone/gelatin electrospun nano fibers for skin tissue regeneration. *Int J Biol Macromol*, 124: 478–491.
166. Liu S, Wang Y, Ming X, *et al.*, 2021, High-speed blow spinning of neat graphene fibrous materials. *Nano Lett*, 21: 5116–5125.
167. McCarthy A, Saldana L, McGoldrick D, *et al.*, 2021, Large-scale synthesis of compressible and re-expandable three-dimensional nanofiber matrices. *Nano Select*, 2: 1566–1579.
168. Jiang Q, Luo B, Wu Z, *et al.*, 2021, Corn stalk/AgNPs modified chitin composite hemostatic sponge with high absorbency, rapid shape recovery and promoting wound healing ability. *J Chem Eng*, 421: 129815.
169. Clasky AJ, Watchorn JD, Chen PZ, *et al.*, 2021, From prevention to diagnosis and treatment: Biomedical applications of metal nanoparticle-hydrogel composites. *Acta Biomater*, 122: 1–25.
170. Zadeh Mehrizi T, Eshghi P, 2021, Investigation of the effect of nanoparticles on platelet storage duration 2010–2020. *Int Nano Lett*, 12:15–45.
171. Kottana RK, Maurizi L, Schnoor B, *et al.*, 2021, Anti-platelet effect induced by iron oxide nanoparticles: Correlation with conformational change in fibrinogen. *Small*, 17: e2004945.
172. Zhao Y, Liu R, Fan Y, *et al.*, 2021, Self-sealing hemostatic and antibacterial needles by polyphenol-assisted surface self-assembly of multifunctional nanoparticles. *J Chem Eng*, 425: 130621.
173. Tao B, Lin C, Yuan Z, *et al.*, 2021, Near infrared light-triggered on-demand Cur release from Gel-PDA@Cur composite hydrogel for antibacterial wound healing. *J Chem Eng*, 403: 126182.
174. Yang Z, Fu X, Zhou L, *et al.*, 2021, Chem-inspired synthesis of injectable metal-organic hydrogels for programmable drug carriers, hemostasis and synergistic cancer treatment. *J Chem Eng*, 423: 130202.
175. Albadawi H, Altun I, Hu J, *et al.*, 2020, Nanocomposite hydrogel with tantalum microparticles for rapid endovascular hemostasis. *Adv Sci*, 8: 2003327.
176. da Silva D, Kaduri M, Poley M, *et al.*, 2018, Biocompatibility, biodegradation and excretion of polylactic acid (PLA) in medical implants and theranostic systems. *J Chem Eng*, 340: 9–14.
177. Song C, Zhang X, Wang L, *et al.*, 2019, An injectable conductive three-dimensional elastic network by tangled surgical-suture spring for heart repair. *ACS Nano*, 13: 14122–14137.
178. Chiong JA, Tran H, Lin Y, *et al.*, 2021, Integrating emerging polymer chemistries for the advancement of recyclable, biodegradable, and biocompatible electronics. *Adv Sci*, 8: e2101233.
179. Ashammakhi N, Hernandez AL, Unluturk BD, *et al.*, 2021, Biodegradable implantable sensors: Materials design, fabrication, and applications. *Adv Funct Mater*, 31: 2104149.
180. Bal-Ozturk A, Cecen B, Avci-Adali M, *et al.*, 2021, Tissue adhesives: From research to clinical translation. *Nano Today*, 36: 101049.
181. Ma C, Sun J, Li B, *et al.*, 2021, Ultra-strong bio-glue from genetically engineered polypeptides. *Nat Commun*, 12: 3613.
182. Li Y, Huang X, Xu Y, *et al.*, 2022, A bio-inspired multifunctional soy protein-based material: From strong underwater adhesion to 3D printing. *J Chem Eng*, 430: 133017.
183. He J, Zhang Z, Yang Y, *et al.*, 2021, Injectable self-healing adhesive pH-responsive hydrogels accelerate gastric hemostasis and wound healing. *Micro Nano Lett*, 13: 80.
184. Poventud-Fuentes I, Kwon KW, Seo J, *et al.*, 2021, A human vascular injury-on-a-chip model of hemostasis. *Small*, 17: e2004889.
185. Kim KY, Ryu JH, Koh MY, *et al.*, 2021, Coagulopathy-independent, bioinspired hemostatic materials A full research story from preclinical models to a human clinical trial. *Sci Adv*, 7: eabc9992
186. Teng L, Shao Z, Bai Q, *et al.*, 2021, Biomimetic glycopolypeptide hydrogels with tunable adhesion and microporous structure for fast hemostasis and highly efficient wound healing. *Adv Funct Mater*, 31: 2105628.
187. Faizullin DA, Valiullina YA, Salnikov VV, *et al.*, 2021, Fibrinogen adsorption on the lipid surface as a factor of regulation of fibrin formation. *Biophysics*, 66: 70–76.
188. Zhou L, Zheng H, Liu Z, *et al.*, 2021, Conductive antibacterial hemostatic multifunctional scaffolds based on ti3c2tx mxene nanosheets for promoting multidrug-resistant bacteria-infected wound healing. *ACS Nano*, 15: 2468–2480.
189. Li Z, Zhao Y, Ouyang X, *et al.*, 2022, Biomimetic hybrid hydrogel for hemostasis, adhesion prevention and promoting regeneration after partial liver resection. *Bioact Mater*, 11: 41–51.
190. Liang Y, Li M, Huang Y, *et al.*, 2021, An integrated strategy for rapid hemostasis during tumor resection and prevention of postoperative tumor recurrence of hepatocellular carcinoma by antibacterial shape memory cryogel. *Small*, 17: e2101356.
191. Mahmoodzadeh A, Moghaddas J, Jarolmasjed S, *et al.*, 2021, Biodegradable cellulose-based superabsorbent as potent hemostatic agent. *J Chem Eng*, 418:129252.
192. Wang Y, Zhao Y, Qiao L, *et al.*, 2021, Cellulose fibers-reinforced self-expanding porous composite with multiple hemostatic efficacy and shape adaptability for uncontrollable massive hemorrhage treatment. *Bioact Mater*, 6: 2089–2104.
193. Lu S, Zhang X, Tang Z, *et al.*, 2021, Mussel-inspired blue-light-activated cellulose-based adhesive hydrogel with fast gelation, rapid haemostasis and antibacterial property for wound healing. *J Chem Eng*, 417: 129329.

194. Peers S, Montebault A, Ladaviere C, 2022, Chitosan hydrogels incorporating colloids for sustained drug delivery. *Carbohydr Polym*, 275: 118689.
195. Kalantari K, Mostafavi E, Saleh B, *et al.*, 2020, Chitosan/pva hydrogels incorporated with green synthesized cerium oxide nanoparticles for wound healing applications. *Eur Polym J*, 134: 109853.
196. Asghari F, Rabiei Faradonbeh D, Malekshahi ZV, *et al.*, 2021, Hybrid PCL/chitosan-PEO nanofibrous scaffolds incorporated with A. euchroma extract for skin tissue engineering application. *Carbohydr Polym*, 278: 118926.
197. Jung HY, Le Thi P, HwangBo KH, *et al.*, 2021, Tunable and high tissue adhesive properties of injectable chitosan based hydrogels through polymer architecture modulation. *Carbohydr Polym*, 261: 117810.
198. Xia L, Wang S, Jiang Z, *et al.*, 2021, Hemostatic performance of chitosan-based hydrogel and its study on biodistribution and biodegradability in rats. *Carbohydr Polym*, 264: 117965.
199. Vakilian S, Jamshidi-Adegani F, Al Yahmadi A, *et al.*, 2021, A competitive nature-derived multilayered scaffold based on chitosan and alginate, for full-thickness wound healing. *Carbohydr Polym*, 262: 117921.
200. Montazerian H, Baidya A, Haghniaz R, *et al.*, 2021, Stretchable and bioadhesive gelatin methacryloyl-based hydrogels enabled by in situ dopamine polymerization. *ACS Appl Mater Interfaces*, 13: 40290–40301.
201. Contessotto P, Orbanic D, Da Costa M, *et al.*, 2021, Elastin-like recombinamers-based hydrogel modulates post-ischemic remodeling in a non-transmural myocardial infarction in sheep. *Sci Transl Med*, 13: eaaz5380.
202. Nelson DW, Gilbert RJ, 2021, Extracellular matrix-mimetic hydrogels for treating neural tissue injury: A focus on fibrin, hyaluronic acid, and elastin-like polypeptide hydrogels. *Adv Healthc Mater*, 10: e2101329.
203. Bai Q, Teng L, Zhang X, *et al.*, 2021, Multifunctional single-component polypeptide hydrogels: The gelation mechanism, superior biocompatibility, high performance hemostasis, and scarless wound healing. *Adv Healthc Mater*, 11: e2101809.
204. Bonito V, Koch SE, Krebber MM, *et al.*, 2021, Distinct effects of heparin and interleukin-4 functionalization on macrophage polarization and in situ arterial tissue regeneration using resorbable supramolecular vascular grafts in rats. *Adv Healthc Mater*, 10: e2101103.
205. Bae S, DiBalsi MJ, Meilinger N, *et al.*, 2018, Heparin-eluting electrospun nanofiber yarns for antithrombotic vascular sutures. *ACS Appl Mater Interfaces*, 10: 8426–8435.
206. Hettiaratchi Marian H, Krishnan L, Rouse T, *et al.*, 2020, Heparin-mediated delivery of bone morphogenetic protein-2 improves spatial localization of bone regeneration. *Sci Adv*, 6: eaay1240.
207. Kucharz K, Kristensen K, Johnsen KB, *et al.*, 2021, Post-capillary venules are the key locus for transcytosis-mediated brain delivery of therapeutic nanoparticles. *Nat Commun*, 12: 4121.
208. Harris AR, Wallace GG, 2017, Organic electrodes and communications with excitable cells. *Adv Funct Mater*, 28: 1700587.
209. Wang K, Frewin CL, Esrafilzadeh D, *et al.*, 2019, High-performance graphene-fiber-based neural recording microelectrodes. *Adv Mater*, 31: e1805867.
210. Maisha N, Rubenstein M, Bieberich CJ, *et al.*, 2021, Getting to the core of it all: nanocapsules to mitigate infusion reactions can promote hemostasis and be a platform for intravenous therapies. *Nano Lett*, 21: 9069–9076.
211. Yang X, Wang C, Liu Y, *et al.*, 2021, Inherent antibacterial and instant swelling  $\epsilon$ -poly-lysine/poly(ethylene glycol) diglycidyl ether superabsorbent for rapid hemostasis and bacterially infected wound healing. *ACS Appl Mater Interfaces*, 13: 36709–36721.
212. Wendels S, Averous L, 2021, Biobased polyurethanes for biomedical applications. *Bioact Mater*, 6: 1083–1106.
213. Xiao M, Yao Y, Fan C, *et al.*, 2021, Multiple H-bonding chain extender-based polyurethane: Ultrasiffness, hot-melt adhesion, and 3D printing finger orthosis. *J Chem Eng*, 433: 133260.
214. Jiang C, Zhang L, Yang Q, *et al.*, 2021, Self-healing polyurethane-elastomer with mechanical tunability for multiple biomedical applications in vivo. *Nat Commun*, 12: 4395.
215. Zhang Z, Zhang Y, Li W, *et al.*, 2021, Curcumin/Fe-SiO<sub>2</sub> nano composites with multi-synergistic effects for scar inhibition and hair follicle regeneration during burn wound healing. *Appl Mater Today*, 23: 101065.
216. Wang Y, Ying T, Li J, *et al.*, 2020, Hierarchical micro/nanofibrous scaffolds incorporated with curcumin and zinc ion eutectic metal organic frameworks for enhanced diabetic wound healing via anti-oxidant and anti-inflammatory activities. *J Chem Eng*, 402: 126273.
217. Liu J, Chen Z, Wang J, *et al.*, 2018, Encapsulation of curcumin nanoparticles with mmp9-responsive and thermos-sensitive hydrogel improves diabetic wound healing. *ACS Appl Mater Interfaces*, 10: 16315–16326.
218. Fahimirad S, Abtahi H, Satei P, *et al.*, 2021, Wound healing performance of PCL/chitosan based electrospun nanofiber electrospayed with curcumin loaded chitosan nanoparticles. *Carbohydr Polym*, 259: 117640.
219. Rao BR, Kumar R, Haque S, *et al.*, 2021, Ag<sub>2</sub>[fe(cn)5no]-fabricated hydrophobic cotton as a potential wound healing dressing: An in vivo approach. *ACS Appl Mater Interfaces*, 13: 10689–10704.
220. Zhang F, Yang H, Yang Y, *et al.*, 2021, Stretchable and biocompatible bovine serum albumin fibrous films supported silver for accelerated bacteria-infected wound healing. *J Chem Eng*, 417: 129145.

221. Xiang J, Zhu R, Lang S, *et al.*, 2021, Mussel-inspired immobilization of zwitterionic silver nanoparticles toward antibacterial cotton gauze for promoting wound healing. *J Chem Eng*, 409: 128291.
222. Chen X, Li H, Qiao X, *et al.*, 2021, Agarose oligosaccharide-silver nanoparticle-antimicrobial peptide-composite for wound dressing. *Carbohydr Polym*, 269: 118258.
223. Kim JW, Mahapatra C, Hong JY, *et al.*, 2017, Functional recovery of contused spinal cord in rat with the injection of optimal-dosed cerium oxide nanoparticles. *Adv Sci*, 4: 1700034.
224. Zhang M, Zhai X, Ma T, *et al.*, 2021, Multifunctional cerium doped carbon dots nanoplatfom and its applications for wound healing. *J Chem Eng*, 423: 130301.
225. Ma X, Cheng Y, Jian H, *et al.*, 2019, Hollow, rough, and nitric oxide-releasing cerium oxide nanoparticles for promoting multiple stages of wound healing. *Adv Healthc Mater*, 8: e1900256.
226. Fan L, Wang W, Wang Z, *et al.*, 2021, Gold nanoparticles enhance antibody effect through direct cancer cell cytotoxicity by differential regulation of phagocytosis. *Nat Commun*, 12: 6371.
227. Zhu GH, Azharuddin M, Islam R, *et al.*, 2021, Innate immune invisible ultrasmall gold nanoparticles—Framework for synthesis and evaluation. *ACS Appl Mater Interfaces*, 13: 23410–23422.
228. Hao F, Liu QS, Chen X, *et al.*, 2019, Exploring the heterogeneity of nanoparticles in their interactions with plasma coagulation factor xii. *ACS Nano*, 13: 1990–2003.
229. Sakoda M, Kaneko M, Ohta S, *et al.*, 2018, Injectable hemostat composed of a polyphosphate-conjugated hyaluronan hydrogel. *Biomacromolecules*, 19: 3280–3290.
230. Sundaram MN, Mony U, Varma PK, *et al.*, 2021, Vasoconstrictor and coagulation activator entrapped chitosan based composite hydrogel for rapid bleeding control. *Carbohydr Polym*, 258:117634.
231. Sun C, Yue P, Chen R, *et al.*, 2022, Chitin-glucan composite sponge hemostat with rapid shape-memory from *Pleurotus eryngii* for puncture wound. *Carbohydr Polym*, 291:119553.
232. Leonhardt EE, Kang N, Hamad MA, *et al.*, 2019, Absorbable hemostatic hydrogels comprising composites of sacrificial templates and honeycomb-like nanofibrous mats of chitosan. *Nat Commun*, 10:1–9.
233. Borges-Vilches J, Figueroa T, Guajardo S, *et al.*, 2022, Novel and effective hemostats based on graphene oxide-polymer aerogels: In vitro and in vivo evaluation. *Biomater Adv*, 139:213007.
234. de Moraes FM, Philippi JV, Belle F, *et al.*, 2022, Lota-carrageenan/xyloglucan/serine powders loaded with tranexamic acid for simultaneously hemostatic, antibacterial, and antioxidant performance. *Biomater Adv*, 137: 212805.